VASCULAR BIOLOGY

Leukotriene B_4 antagonism ameliorates experimental lymphedema

Wen Tian,[1,2]* Stanley G. Rockson,[2]*† Xinguo Jiang,[1,2]* Jeanna Kim,[2]* Adrian Begaye,[2] Eric M. Shuffle,[1,2] Allen B. Tu,[1,2] Matthew Cribb,[3] Zhanna Nepiyushchikh,[3] Abdullah H. Feroze,[2] Roham T. Zamanian,[2] Gundeep S. Dhillon,[2] Norbert F. Voelkel,[4] Marc Peters-Golden,[5] Jan Kitajewski,[6] J. Brandon Dixon,[3] Mark R. Nicolls[1,2]*†

Acquired lymphedema is a cancer sequela and a global health problem currently lacking pharmacologic therapy. We have previously demonstrated that ketoprofen, an anti-inflammatory agent with dual 5-lipoxygenase and cyclooxygenase inhibitory properties, effectively reverses histopathology in experimental lymphedema. We show that the therapeutic benefit of ketoprofen is specifically attributable to its inhibition of the 5-lipoxygenase metabolite leukotriene B_4 (LTB_4). LTB_4 antagonism reversed edema, improved lymphatic function, and restored lymphatic architecture in the murine tail model of lymphedema. In vitro, LTB_4 was functionally bimodal: Lower LTB_4 concentrations promoted human lymphatic endothelial cell sprouting and growth, but higher concentrations inhibited lymphangiogenesis and induced apoptosis. During lymphedema progression, lymphatic fluid LTB_4 concentrations rose from initial prolymphangiogenic concentrations into an antilymphangiogenic range. LTB_4 biosynthesis was similarly elevated in lymphedema patients. Low concentrations of LTB_4 stimulated, whereas high concentrations of LTB_4 inhibited, vascular endothelial growth factor receptor 3 and Notch pathways in cultured human lymphatic endothelial cells. Lymphatic-specific *Notch1*$^{-/-}$ mice were refractory to the beneficial effects of LTB_4 antagonism, suggesting that LTB_4 suppression of Notch signaling is an important mechanism in disease maintenance. In summary, we found that LTB_4 was harmful to lymphatic repair at the concentrations observed in established disease. Our findings suggest that LTB_4 is a promising drug target for the treatment of acquired lymphedema.

INTRODUCTION

Lymphedema is a state of vascular functional insufficiency in which decreased lymphatic clearance of interstitial fluid leads to edema formation and progressive, debilitating architectural alterations of the skin and supporting tissues (*1*). Primary lymphedema occurs infrequently on an idiopathic or heritable basis [for example, Milroy's disease, due to a missense inactivating mutation of vascular endothelial growth factor receptor 3 (*Vegfr3*)]. Secondary lymphedema, by distinction, is the result of acquired damage to the lymphatic vasculature, such as occurs after lymph node resection and radiotherapy in cancer patients or after parasitic infection (*2*). Acquired lymphedema affects 15 to 50% of cancer survivors, and lymphatic filariasis with lymphedema afflicts an estimated 90 million individuals globally (*2*).

Lymphedema is characterized by the nonresolving accumulation of protein-rich interstitial fluid, the presence of a significant inflammatory cell infiltrate, and dysregulated regional immune responses. Subsequent adipose tissue deposition and fibrosis promote progressive anatomic distortion and loss of function in the affected areas (*2*). Current treatments, including physiotherapy and the use of compression garments, only transiently decrease edema and do not substantially prevent the tissue destruction that may accompany the more advanced stages of disease; pharmacotherapeutic options remain extremely limited and largely ineffective (*3*). We previously demonstrated that ketoprofen, a nonsteroidal anti-inflammatory drug (NSAID) typically used as a pain reliever, reversed the edema and structural alterations of experimental lymphedema; this preclinical study led to a randomized, blinded, placebo-controlled clinical trial that tests this agent in human disease (NCT02257970), which is now fully enrolled and awaiting completion (*4*). Unfortunately, ketoprofen has gastrointestinal, cardiac, nervous system, renal, and hepatic toxicities, which potentially limit its long-term use, and safer, more targeted therapies will be necessary for amelioration and stabilization of this chronic disease.

The mechanism by which ketoprofen ameliorates lymphedema is unknown (*5*–*7*). Ketoprofen, an NSAID inhibitor of cyclooxygenase (COX), has a relatively unique pharmacology within its class, insofar as it also inhibits 5-lipoxygenase (5-LO) (*5*–*7*). 5-LO oxygenates arachidonic acid to yield an unstable intermediate, leukotriene A_4 (LTA_4). LTA_4 is quickly converted by LTA_4 hydrolase (LTA_4H) to LTB_4 or, alternatively, by LTC_4 synthase (LTC_4S) to the cysteinyl leukotrienes (cysLTs) (LTC_4, LTD_4, and LTE_4) (*8*). The dual inhibitory property of ketoprofen implies that the efficacy of ketoprofen in experimental lymphedema might be mediated by its capacity to inhibit either or both of these two pathways of arachidonic acid metabolism.

The murine model of subacute, acquired lymphedema closely simulates the volume responses, histopathology, immune trafficking, and lymphoscintigraphic characteristics of acquired human lymphedema (*9*), and the cutaneous inflammatory responses observed in mouse tail lymphedema replicate those of acquired lymphedema in humans (*10*). Using this model along with the studies that adopted human lymphatic endothelial cell (HLEC) culture, we found that although lower LTB_4 concentrations promoted lymphatic sprouting and growth in vitro, higher concentrations inhibited lymphangiogenesis and induced apoptosis of HLECs. After lymphatic ablation, lymph LTB_4 concentrations were initially in the prolymphangiogenic range but rose, over subsequent days, into an antilymphangiogenic range. Low concentrations of LTB_4 stimulated, whereas higher concentrations observed in lymphedema state inhibited, VEGFR3 and Notch pathways in LECs. Lymphatic-specific

[1]VA Palo Alto Health Care System, Palo Alto, CA 94304, USA. [2]Stanford University School of Medicine, Stanford, CA 94305, USA. [3]Georgia Institute of Technology, Atlanta, GA 30332, USA. [4]Virginia Commonwealth University, Richmond, VA 23284, USA. [5]University of Michigan Health Systems, Ann Arbor, MI 48109, USA. [6]University of Illinois at Chicago, Chicago, IL 60612, USA.
*These authors contributed equally to this work.
†Corresponding author. Email: rockson@stanford.edu (S.G.R.); mnicolls@stanford.edu (M.R.N.)

Notch1$^{-/-}$ mice did not benefit from LTB_4 antagonism, consistent with a critical role for LTB_4 suppression of Notch signaling as a mechanism of disease propagation.

RESULTS

Ketoprofen efficacy in a preclinical model of lymphedema can be attributed to its inhibition of LTB_4

Whereas sham surgery (sham), which involves tail skin incision only, does not cause tail lymphedema, lymphatic ablation surgery (lymphatic surgery) leads to progressive tail swelling and associated structural alterations (Fig. 1, A and B, and fig. S1). Lymphedema in this model is characterized by a disease progression phase during the first 2 weeks with minimal resolution over the subsequent weeks (Fig. 1B). To help determine whether ketoprofen's therapeutic effects in lymphedema depended on its ability to inhibit COX and/or 5-LO pathways of arachidonate metabolism, we used pharmacologic agents that block COX (ibuprofen), 5-LO (zileuton), CysLT1 (montelukast), LTA_4H (bestatin), and the LTB_4 receptor BLT1 (Ly293111 and lentiviral sh*Ltb4r1*) (Fig. 1C). Although ibuprofen and montelukast were ineffective, therapies that decreased the biosynthesis of LTB_4 (ketoprofen, zileuton, and bestatin) or its signaling via the high-affinity receptor BLT1 (Ly293111 and sh*Ltb4r1*) effectively reversed tail edema, dermal/epidermal thickening, and lymphatic dilation (Fig. 1, D to M, and fig. S2). These results demonstrate that the efficacy of ketoprofen for the treatment of lymphedema is likely attributable to its inhibitory effects on LTB_4 signaling.

LTB_4 antagonism leads to improved tail anatomy, better lymphatic clearance, diminished tissue inflammation, and improved blood vessel integrity

To evaluate the effects of LTB_4 antagonism on mouse tail lymphatic anatomy and function, we compared bestatin-treated groups with both saline-treated lymphatic ablation surgery controls and sham surgery controls. Relative to saline-treated animals, bestatin therapy conferred a relatively thinner dermis and epidermis while better preserving the epidermal/dermal junction (Fig. 2A). Fluorescence microlymphangiography of mice with red fluorescence tied to the expression of the LEC marker Prox1 (*Prox1-Cre-ERT2-tdTomato* mice) revealed dilated and poorly draining lymphatics in the diseased reporter mice, which were effectively restored by bestatin treatment (Fig. 2B). We further quantified the lymphatic function using a novel technology integrating a NIR imaging system with a controlled pressure cuff to modulate lymph flow (*11*, *12*). In the bestatin-treated mice, NIR identified lymph flow successfully passed beyond the surgical wound and filled the proximal lymphatic collectors, whereas minimal NIR transportation was seen in the saline-treated lymphedema animals (Fig. 2, C and D, and movies S1 to S3). Extravasation of Evans Blue dye proximal to the wound indicated increased permeability of the lymphatics in the saline-treated group, which was attenuated by bestatin therapy (Fig. 2E). These results corroborate the microlymphangiography data and support the restorative effects of bestatin therapy after injury. Bestatin treatment also resulted in diminished macrophage and neutrophil infiltration within the tail skin evaluated 24 days after lymphatic ablation (fig. S3, A and B). Bestatin treatment reduced the concentrations of interleukin-6 (IL-6), IL-4, IL-13, and IL-17A similar to control values but significantly elevated IL-10 above saline-treated mice with lymphedema (fig. S3C). Macrophage depletion with clodronate, despite delaying lymphedema, was not sufficient to reverse the disease at day 24 (fig. S4). Consistent with the documented protective effects of bestatin on vascular endothelium (*13*), microvascular leakage was also attenuated by treatment of this drug (fig. S5).

LTB_4 exhibits concentration-dependent effects on HLEC lymphangiogenesis and survival

Because the effects of LTB_4 on the structure and function of lymphatic circulation have not been previously investigated, we assessed how this eicosanoid affected HLECs in several in vitro and in vivo lymphangiogenesis assays. LTB_4 exhibited bimodal effects on network formation, fibrin gel sprouting, and three-dimensional (3D) spheroid sprouting assays (Fig. 3, A to E). Lower LTB_4 concentrations in the 1 to 10 nM range were prolymphangiogenic with enhanced network length after 12 hours (Fig. 3B), and more and longer lymphatic protrusions in the fibrin gel and spheroid assays were observed after 3 days of culture (Fig. 3, C to E). Higher LTB_4 concentrations in the 200 to 400 nM range were antilymphangiogenic and induced HLEC death, which can readily be seen in the fibrin gel and spheroid assays (Fig. 3A). The deleterious effects of HLECs cultured under the 200 to 400 nM LTB_4 conditions directly contrast with the prolymphangiogenic effects of VEGF-C in parallel lymphangiogenesis assays (Fig. 3, F to I). Additionally, the antilymphangiogenic actions of 400 nM LTB_4 could be reversed by blocking LTB_4 signaling, using the BLT1 antagonist U75302 or sh*Ltb4r1* (Fig. 3, F to I, and fig. S6, A and B). By distinction, 400 nM LTC_4 did not affect lymphangiogenesis, whereas the COX1/2 metabolite prostaglandin E_2 (PGE_2) promoted lymphangiogenesis (fig. S6, C to E). To determine the in vivo effects of high LTB_4 concentration, we used a Matrigel plug assay, using HLECs in severe combined immunodeficient (SCID) mice. Here, 400 nM LTB_4 attenuated lymphatic vessel formation in vivo, whereas blocking LTB_4 signaling restored lymphatic vessel growth (Fig. 3J and fig. S6F). To further test whether LTB_4 also exerted a bimodal functionality for HLEC survival, we conducted a triplex assay to gauge HLEC viability, cytotoxicity, and apoptosis and found enhanced viability in the 2 to 10 nM range of LTB_4 and increased cytotoxicity/apoptosis in the 200 to 400 nM range (Fig. 3K). Increased HLEC apoptosis at concentrations of 200 to 400 nM LTB_4 was confirmed by Western blot analysis of cleaved caspase 3 (Fig. 3L). However, although the evidence clearly indicates prolymphangiogenic effects of LTB_4 in the 2 to 10 nM range, it is unclear whether such low concentrations of LTB_4 directly cause LEC proliferation. Because the lymphatic system is characterized by distinct endothelial-cellular junctions to facilitate fluid, macromolecule, and cell transport, we evaluated the expression of various junctional proteins after 400 nM LTB_4 treatment. Immunofluorescence staining for VE-cadherin revealed that this high concentration of LTB_4 damaged HLEC adherens junctions (fig. S7A). Similarly, mRNA transcripts of gap junctional proteins connexin 37, 43, and 47 were reduced in the LTB_4-treated cells (fig. S7B). Cumulatively, these results suggest that LTB_4 exhibits divergent actions that promote lymphangiogenesis at lower concentrations but impede lymphatic growth and function at higher concentrations.

LTB_4 production is elevated in preclinical and clinical lymphedema

To assess the kinetics of LTB_4 production in lymphedema, we measured LTB_4 in the mouse tail lymphatics over time (Fig. 4A). During the first 3 days after lymphatic ablation, LTB_4 concentrations were within the prolymphangiogenic range, as defined in Fig. 3. Notably, as disease progressed and intensified, LTB_4 rose into a range congruent with antilymphangiogenic concentrations. Serum LTB_4 concentrations were also elevated in the diseased mice (Fig. 4B). This trend was matched by a corresponding increase in *Ltb4r1* tissue expression

(Fig. 4C). 5-LO expression was prominent in macrophages and neutrophils in the lymphedematous mouse tail skin (Fig. 4D and fig. S3B). Adult patients with a spectrum of acquired and primary lymphedema were assessed, including those with upper and lower extremity edema, both related and unrelated to a cancer diagnosis. Increased LTB_4 concentrations were detected in the serum of these patients, and augmented activation of 5-LO in local immune infiltrates was observed (Fig. 4, E and F, and fig. S8). *Prox1-Cre-ERT2-tdTomato* reporter mice demonstrated increased lymphatic endothelial LTA_4H and decreased COX2 and microsomal prostaglandin E synthase-1 (mPGES-1) tissue expression (fig. S9, A to C), whereas bestatin treatment restored the expression of these enzymes. Serum PGE_2 concentrations were decreased both in lymphedema mice and in patients (fig. S9D and table S1). These findings suggest that lymphedema pathology is associated with an imbalanced eicosanoid metabolism: activated LTB_4 biosynthesis but diminished PGE_2 production.

Blocking LTB_4 during the early lymphangiogenesis period abrogates the therapeutic effect of LTB_4 antagonism

It has been previously established that after lymphatic ablation, lymphangiogenesis occurs during the first 3 days after surgery; the degree to which this occurs may serve to limit the extent of lymphedema development (*14*). This early lymphangiogenic response corresponds to the time interval in which the amount of LTB_4 in lymphatic fluid is

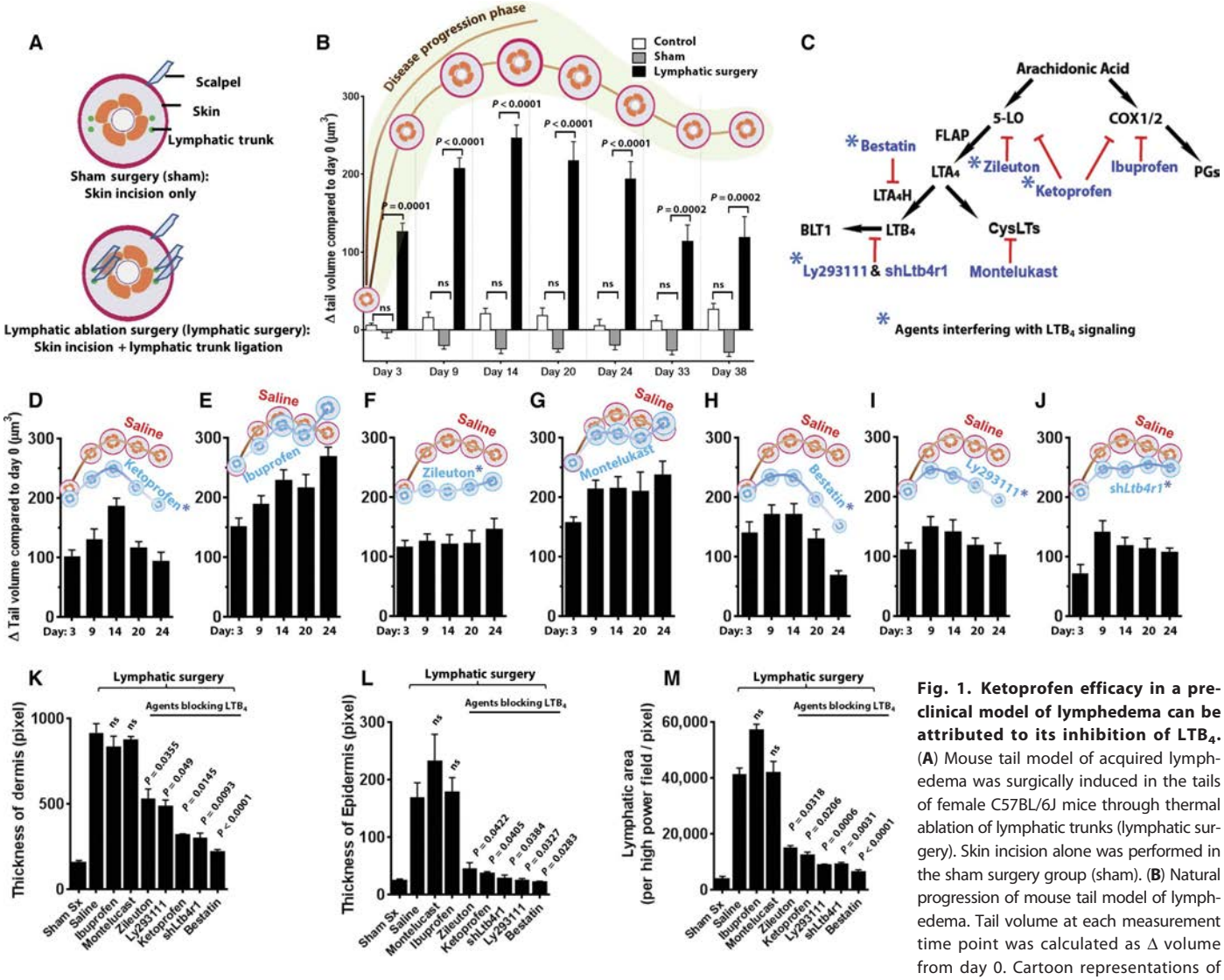

Fig. 1. Ketoprofen efficacy in a preclinical model of lymphedema can be attributed to its inhibition of LTB_4. (**A**) Mouse tail model of acquired lymphedema was surgically induced in the tails of female C57BL/6J mice through thermal ablation of lymphatic trunks (lymphatic surgery). Skin incision alone was performed in the sham surgery group (sham). (**B**) Natural progression of mouse tail model of lymphedema. Tail volume at each measurement time point was calculated as Δ volume from day 0. Cartoon representations of the cross-sectional view of lymphedematous tails were created to illustrate lymphedema progression. Mice without surgery (control) or sham groups were compared to the categories subjected to lymphatic surgery; $n = 8$. (**C**) Overview of the eicosanoid pathway. Therapies, targeting different eicosanoid pathways, tested in the study were marked in blue. (**D** to **J**) Serial tail volume measurements at each time point over 24 days. Treatments targeting both 5-LO and COX1/2 (ketoprofen, $n = 15$) (D), 5-LO (zileuton, $n = 10$) (F), LTA_4H (bestatin, $n = 14$) (H), BLT1 (Ly293111, $n = 10$) (I), or *Ltb4r1* (local administering of lentiviral sh*Ltb4r1*, $n = 6$) (J) were compared with ibuprofen (inhibits COX1/2, $n = 13$) (E) and montelukast (antagonizes CysLT, $n = 10$) (G) therapies. All therapies started on postsurgical day 3. Cartoon representations in red demonstrate the cross-sectional view of the lymphedematous tails in the saline-treated groups; cartoon in blue illustrates the eicosanoid inhibitor–treated animals after lymphatic ablation. Quantification of dermal (**K**) and epidermal (**L**) skin thickness and lymphatic area (**M**) in the day 24 mouse tail skin for (D) to (J); $n = 5$. In (B) and (D) to (M), data are presented as means and SEM; ns, not significant, Kruskal-Wallis test followed by Dunn's multiple comparisons test for post hoc analyses.

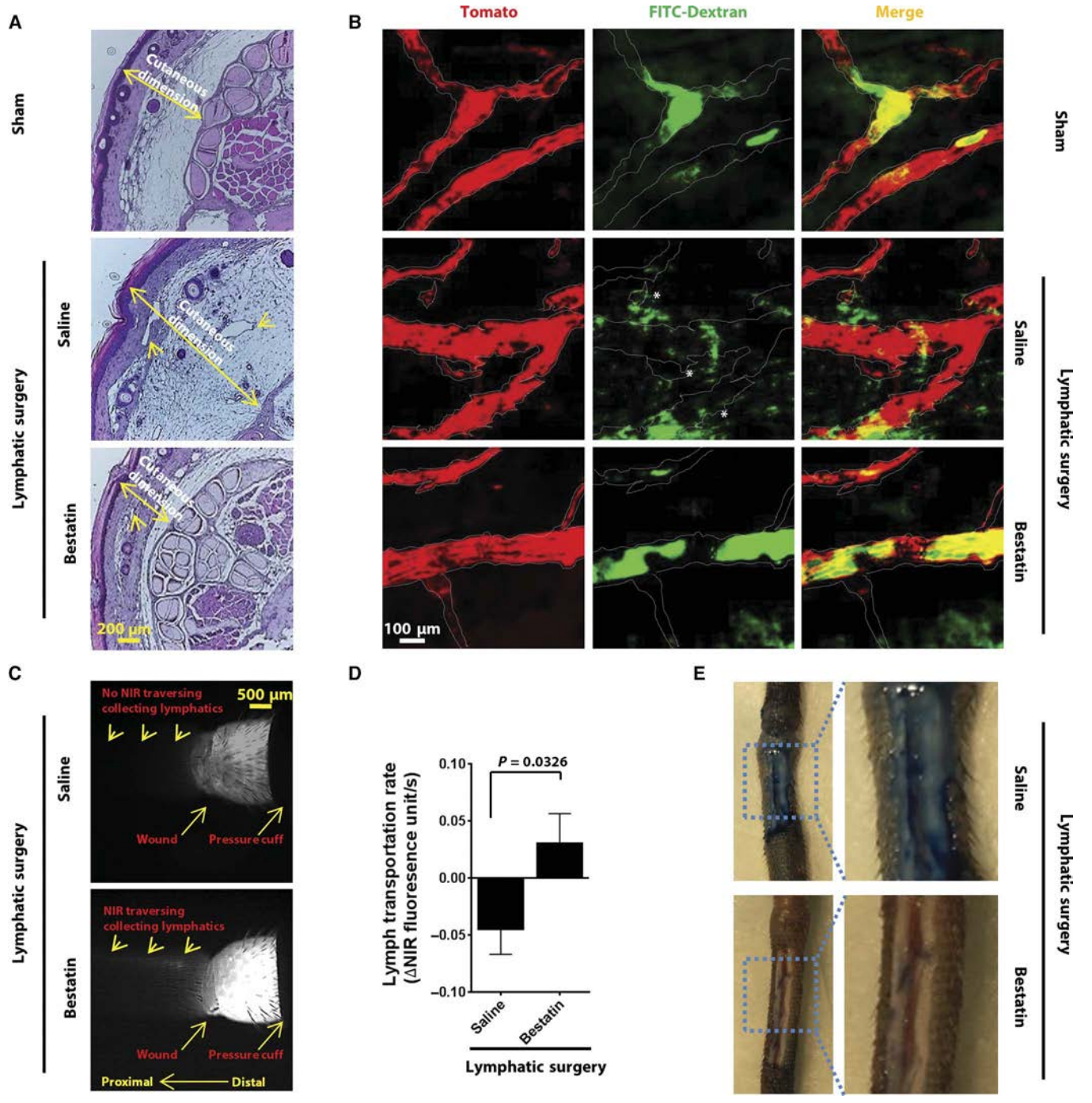

Fig. 2. Bestatin treatment improves tail anatomy and restores lymphatic function. (**A**) Representative histology of mouse tail harvested on day 24 comparing samples from sham surgery control (sham) and animals treated with saline or bestatin after lymphatic ablation surgery (lymphatic surgery). Yellow arrowheads point at lymphatic dilation. Cutaneous dimension is indicated by yellow arrows. Scale bar, 200 μm; $n = 6$. (**B**) Fluorescence dextran microlymphangiography in the *Prox1-Cre-ERT2-tdTomato* mouse tail. Lymphatics are genetically marked by tdTomato (red) and outlined with a white dashed line. Fluorescein isothiocyanate (FITC)–dextran is shown in green. FITC-dextran not taken up by lymphatics is indicated by a white asterisk. Scale bar, 100 μm; $n = 5$. (**C**) Representative still photographs from movies S2 and S3 captured by a near-infrared (NIR) imaging system with a controlled pressure cuff. The collecting lymphatic function was tracked by imaging the transportation of a NIR dye in the vessels. Collecting lymphatics and the surgical wound are marked. Direction of lymph flow from the distal to the proximal part of the mouse tail is indicated. Scale bar, 500 μm; $n = 3$. (**D**) Trafficking ability of collecting lymphatics as quantified by the rate of NIR packet movement; $n = 3$; data are presented as means and SEM, Mann-Whitney test. (**E**) Representative images showing extravasation of Evans Blue dye from the lymphatics distal to the wound in the saline-treated mouse tail after lymphatic surgery; $n = 3$.

within the prolymphangiogenic range (Figs. 3 and 4A). Thus, the effects that congenital absence of 5-LO or BLT1 would have in this model remain to be established. To address this question, we examined lymphedema in *Alox5*$^{-/-}$ and *Ltb4r1*$^{-/-}$ mice (mice with a global gene deletion of 5-LO or BLT1). Both experimental groups developed tail edema and skin lesions after lymphatic and sham surgery (Fig. 5, A and B, and fig. S10, A and B). Therefore, we hypothesized that LTB_4 signaling played an important functional role in the initial lymphangiogenesis period and that blocking LTB_4 during this phase was potentially deleterious, in contrast to the therapeutic effects of antagonizing LTB_4 3 days after lymphatic ablation. This notion is consistent with the recent observation that blocking LTB_4 with bestatin on day 1 after wounding results in significantly larger skin lesions (*15*, *16*). To confirm a prolymphangiogenic function of LTB_4 in the initial lymphangiogenesis period, local sh*Ltb4r1* lentiviral injection, bestatin, and Ly293111 therapies were administered to the wild-type (WT) mice before sham and lymphatic surgery. None of these strategies for antagonizing LTB_4 before the initial lymphangiogenesis period helped to resolve lymphatic injury (Fig. 5, C to E, and fig. S10, C to E), with dermal thickness and lymphatic dilation remaining unimproved 24 days after surgery (Fig. 5, F and G). Figure 5H and fig. S10F illustrate the marked differences in clinical outcomes based on the timing of when LTB_4 signaling is abrogated (that is, before or after the initial lymphangiogenesis period). Additionally, once LTB_4 concentrations climbed into the antilymphangiogenic range, blockade of LTB_4 synthesis (started on day 3, day 9, or day 14) was therapeutic (fig. S10G).

To mechanistically explore why LTB_4 antagonism was not protective before the initial lymphangiogenesis period, we evaluated the expression of 168 pertinent lymphangiogenic and angiogenic genes in *Alox5*$^{-/-}$ mice 1, 2, and 3 days after sham or lymphatic surgery and found significant down-regulation of key lymphangiogenic and angiogenic genes in both surgery groups (table S2). On the basis of the transcriptomic evidence of defective lymphangiogenesis in *Alox5*$^{-/-}$ mice, we studied how LTB_4 antagonism affected mouse tail lymphangiogenic gene expression before and after the initial lymphangiogenesis period. In mice subjected to LTB_4 antagonism before the initial lymphangiogenesis period (*Alox5*$^{-/-}$ mice and WT mice with sh*Ltb4r1* pretx), key lymphangiogenic genes were down-regulated (Fig. 5I, decreased average fold change is highlighted in red). In mice in which LTB_4 antagonism with bestatin and sh*Ltb4r1* was started on day 3, these same genes were up-regulated (Fig. 5I, increased fold change is highlighted in green). Collectively, these data imply an important temporal aspect

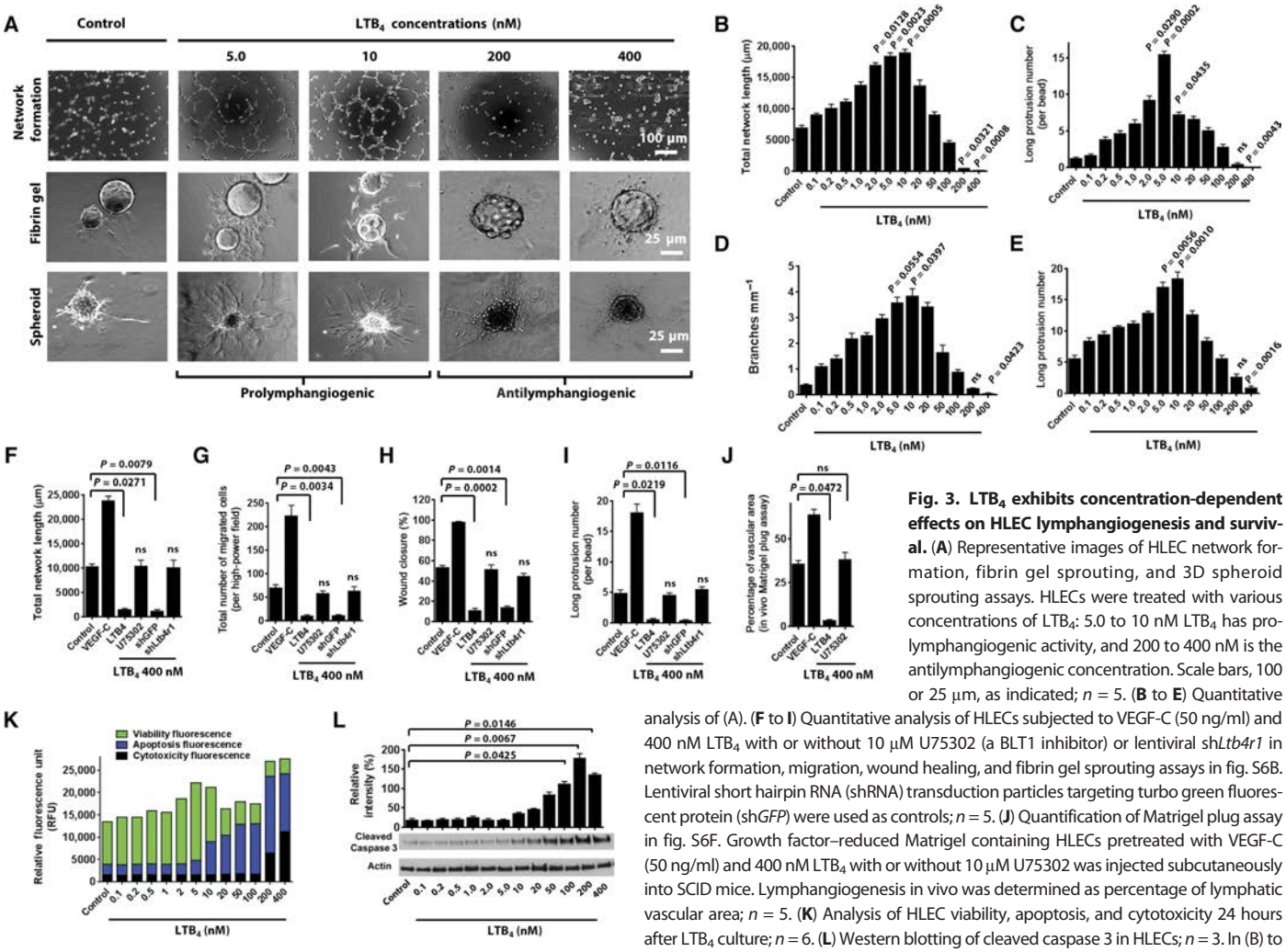

Fig. 3. LTB_4 exhibits concentration-dependent effects on HLEC lymphangiogenesis and survival. (**A**) Representative images of HLEC network formation, fibrin gel sprouting, and 3D spheroid sprouting assays. HLECs were treated with various concentrations of LTB_4: 5.0 to 10 nM LTB_4 has prolymphangiogenic activity, and 200 to 400 nM is the antilymphangiogenic concentration. Scale bars, 100 or 25 μm, as indicated; $n = 5$. (**B** to **E**) Quantitative analysis of (A). (**F** to **I**) Quantitative analysis of HLECs subjected to VEGF-C (50 ng/ml) and 400 nM LTB_4 with or without 10 μM U75302 (a BLT1 inhibitor) or lentiviral sh*Ltb4r1* in network formation, migration, wound healing, and fibrin gel sprouting assays in fig. S6B. Lentiviral short hairpin RNA (shRNA) transduction particles targeting turbo green fluorescent protein (sh*GFP*) were used as controls; $n = 5$. (**J**) Quantification of Matrigel plug assay in fig. S6F. Growth factor–reduced Matrigel containing HLECs pretreated with VEGF-C (50 ng/ml) and 400 nM LTB_4 with or without 10 μM U75302 was injected subcutaneously into SCID mice. Lymphangiogenesis in vivo was determined as percentage of lymphatic vascular area; $n = 5$. (**K**) Analysis of HLEC viability, apoptosis, and cytotoxicity 24 hours after LTB_4 culture; $n = 6$. (**L**) Western blotting of cleaved caspase 3 in HLECs; $n = 3$. In (B) to (J) and (L), data are presented as means and SEM; comparisons with the control groups were made using Kruskal-Wallis test followed by Dunn's multiple comparisons test for post hoc analyses. In (K), mean fluorescence readings are shown.

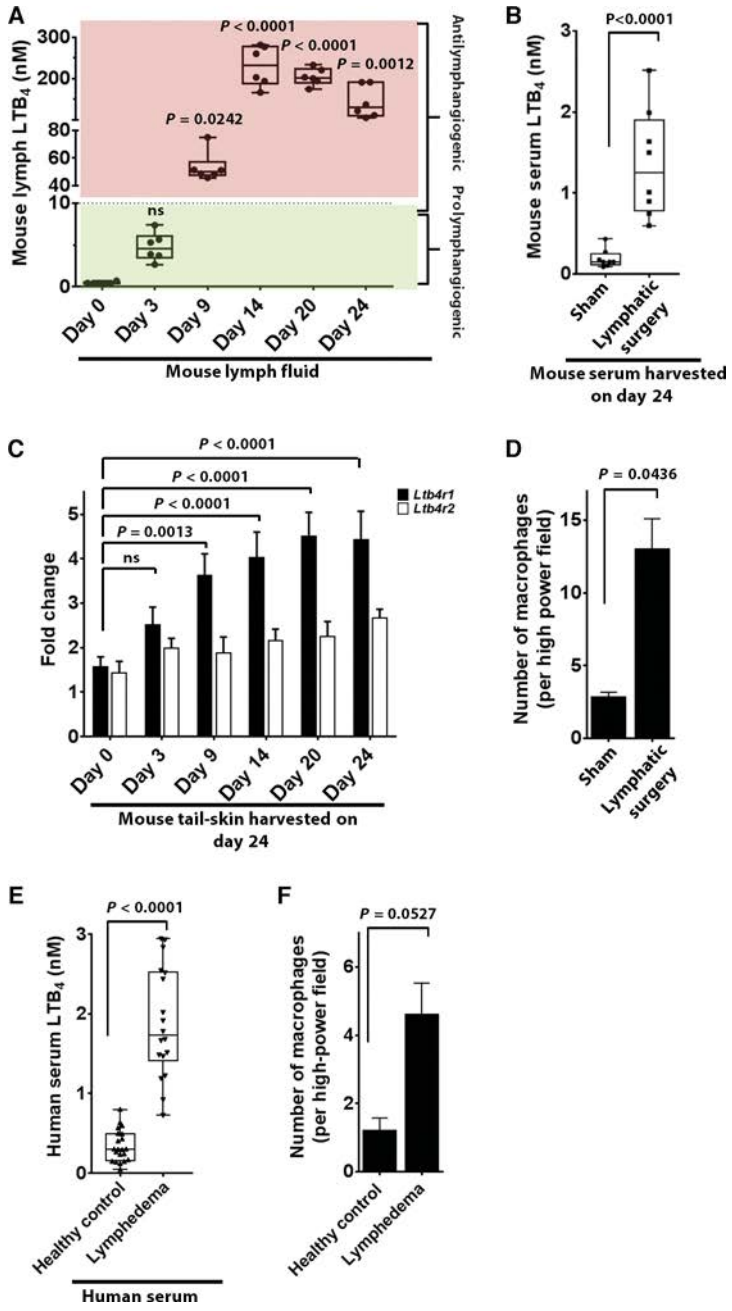

Fig. 4. LTB_4 production is elevated in preclinical and clinical lymphedema. (**A**) LTB_4 concentrations in the lymph fluid, measured by liquid chromatography–tandem mass spectrometry (LC-MS/MS) over time as mouse tail lymphedema developed; $n = 6$. (**B**) Mouse serum LTB_4 concentrations, measured by LC-MS/MS. Blood serum was collected on postsurgical day 24; $n = 6$. (**C**) Transcripts of *Ltb4r1* and *Ltb4r2* in the tail skin, measured by quantitative reverse transcription polymerase chain reaction (qRT-PCR); $n = 5$. (**D**) Quantification of 5-LO–positive macrophages in the mouse tail skin in fig. S3B; $n = 5$. (**E**) LTB_4 concentrations in the blood serum of healthy controls ($n = 21$) and lymphedema ($n = 18$) patients, measured by LC-MS/MS. Demographic data are shown in table S1. (**F**) Quantification of 5-LO–expressing macrophages in patient skin samples in fig. S8; $n = 5$. For (A), (B), and (E), data are presented in box-and-whiskers plots showing minimal to maximal values and all data points; for (C), (D), and (F), data are presented as means and SEM; comparisons with day 0 samples in (A) and (C) were made using Kruskal-Wallis test followed by Dunn's multiple comparisons test for post hoc analyses; comparisons as indicated in (B), (D), (E), and (F) used the Mann-Whitney test.

of LTB_4 signaling, underscoring the beneficial role of lower concentrations LTB_4 during the early phase of lymphatic growth. By contrast, when LTB_4 concentrations markedly rise during the evolution of the experimental disease, the influence of LTB_4 shifts toward a deleterious role.

LTB_4 exerts concentration-dependent effects on VEGFR3 and Notch signaling

Because the bimodal effects of LTB_4 on lymphangiogenesis have not been previously reported, we next investigated the pathways putatively altered by LTB_4 in HLECs. We evaluated two key pathways implicated in lymphangiogenesis: VEGFR3 and Notch (*17*). At low concentrations (5 to 10 nM), LTB_4 increased the mRNA and protein expression and phosphorylation of VEGFR3 and VEGFR2. By contrast, high concentrations of LTB_4 (200 to 400 nM) inhibited these parameters (Fig. 6, A to C, and fig. S11). Injection of adenovirus-overexpressing 5-LO (Ad5-LO) to the WT mouse tail resulted in impaired lymphatic drainage, excessive lymphatic sprouting, and microvascular leakage that were commonly associated with nonproductive lymphangiogenesis in lymphedema (fig. S12). These results collectively demonstrate that, similar to its effects on lymphangiogenesis itself, LTB_4 exerts bimodal actions on lymphatic VEGFR3 and VEGFR2 signaling. We then examined whether LTB_4 exerted a similar concentration-dependent regulation of the Notch pathway using a CSLx6 reporter assay (*18*) and showed diminished luciferase activity only at higher LTB_4 concentrations (200 to 400 nM) (Fig. 6D). LTB_4 inhibition of Notch signaling was abrogated by pretreatment of BLT1 shRNA and was reversed by the addition of Dll4 (a Notch ligand), indicating that LTB_4 inhibited Notch signaling specifically through the BLT1 receptor (Fig. 6E). Western blot analysis of Dll4 and Notch intracellular domain (NICD) corroborated the luciferase assay results (fig. S13A). PCR measurements of Notch target genes *EFNB2*, *Hes1*, and *Hey1* were also consistent with the reporter assay findings (Fig. 6, F to H). Because Notch signaling is strongly associated with the endothelial stalk cell phenotype (*19*–*23*) and assessment of the nuclear localization of NICD is an established approach for determining the activation of Notch, NICD and filopodia histology of HLECs was evaluated. Both DAPT (an inhibitor of canonical Notch pathway) and LTB_4 (200 nM) treatment resulted in increased filopodia and decreased nuclear-localized NICD, suggesting a down-regulation of Notch activity (fig. S13B). sh*Ltb4r1*- and Dll4-treated HLECs repealed the LTB_4-mediated, Notch inhibition–associated tip cell phenotype and instead displayed a unified stalk cell shape with enhanced NICD nuclear localization (fig. S13B). These in vitro data collectively demonstrate that LTB_4 promoted VEGFR3 at low concentrations (5 to 10 nM) and inhibited both VEGFR3 and Notch signaling at high concentrations (200 to 400 nM).

Bimodal effects of LTB_4 on lymphangiogenesis are regulated by VEGFR3 and Notch signaling

We next investigated the role of VEGFR3 and Notch signaling in the bimodal effects of LTB_4 on lymphangiogenesis and HLEC survival. At a concentration of 5 nM, which increased VEGFR3 expression and activation (Fig. 6, A and B), LTB_4 promoted HLEC sprouting; blocking BLT1 with sh*Ltb4r1* or blocking

VEGFR3 with the kinase inhibitor Maz51 neutralized its prolymphangiogenic effects (Fig. 7, A to D). At a concentration of 200 nM, which inhibited VEGFR3 expression and phosphorylation (Fig. 6, A and B), LTB_4 blocked HLEC sprouting; inhibiting BLT1 or adding VEGF-C neutralized its antilymphangiogenic effects (Fig. 7, A to D). Recombinant Dll4 rescued HLEC Notch signaling from 200 nM LTB_4 treatment (Fig. 6, E to J), but it did not completely restore HLEC sprouting, suggesting that LTB_4-mediated inhibition of VEGFR3 is likely a more important determinant of its antilymphangiogenic activity than its inhibition of the Notch pathway (Fig. 7, A to D). Because VEGFR3 and Notch are both essential for HLEC survival (*18*, *24*), we next evaluated the role of each pathway on LTB_4-mediated cell prosurvival effects noted at lower LTB_4 concentrations as well as on LTB_4-mediated injury seen at higher concentrations. Inhibiting BLT1 (via sh*Ltb4r1*) or VEGFR3 (via Maz51) reversed the proproliferative response induced by 5 nM LTB_4 (Fig. 7E). Dll4, VEGF-C, and sh*Ltb4r1* prevented 200 nM LTB_4–induced HLEC apoptosis. These results suggest that LTB_4 regulates lymphangiogenesis and HLEC survival through differential regulation of VEGFR3 and Notch pathways.

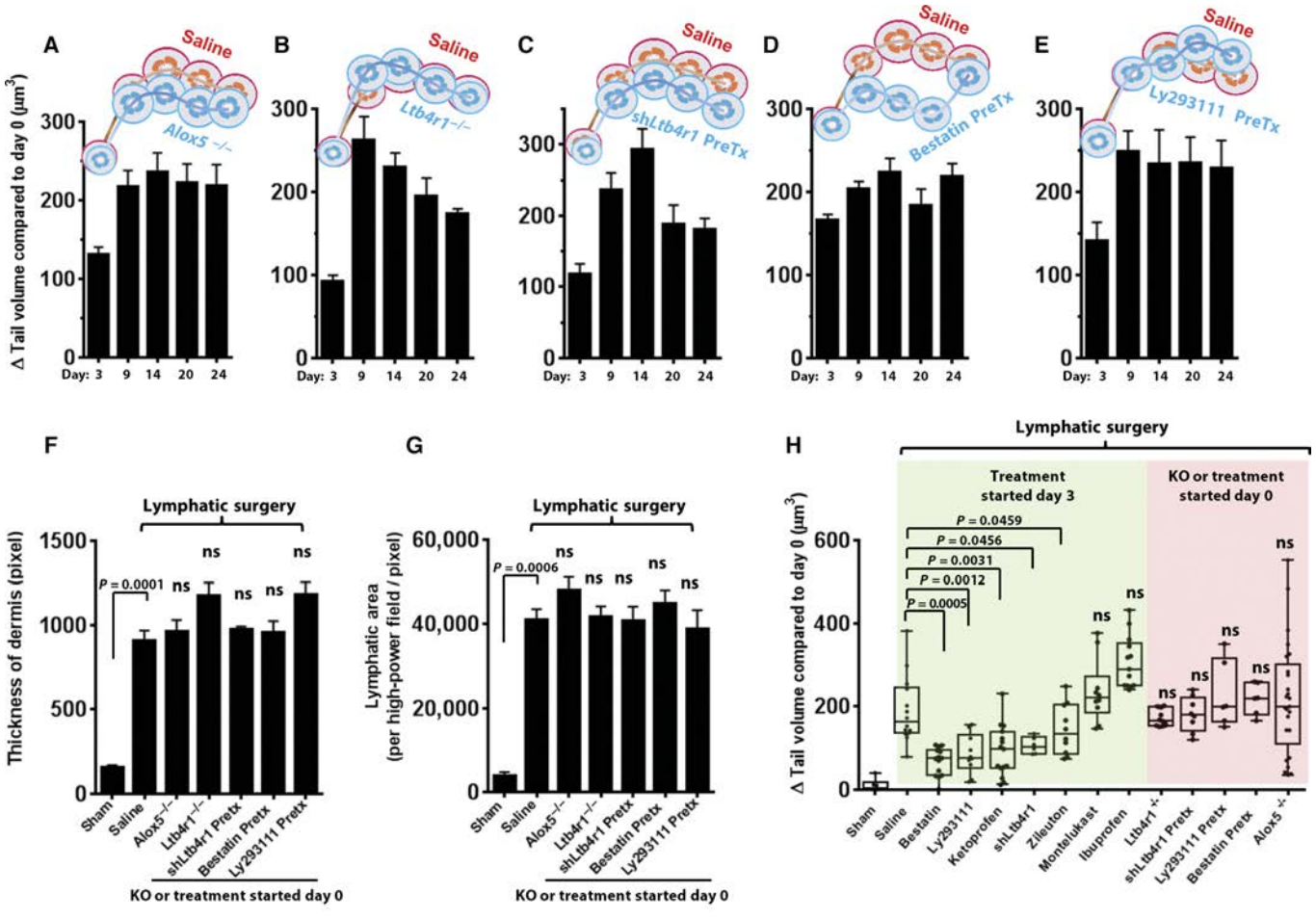

I

Effect of LTB_4 antagonism timing on lymphangiogenic gene expression in mouse tail skin									
LTB_4 antagonism group		Genes							
		Angpt1	*Angpt2*	*Tie2*	*Vegfr3*	*Vegfr2*	*Mmp9*	*Nrp1*	*Nrp2*	*S1pR1*
Treatment before initial lymphangiogenesis period	$Alox5^{-/-}$	8.3	2.4	20.0	6.9	6.6	10.5	2.8	3.2	2.9
	sh*Ltb4r1* Pretx	8.5	1.9	7.9	5.0	4.4	8.6	3.8	3.5	2.4
Treatment after initial lymphangiogenesis period	Bestatin	1.9	1.5	2.3	2.8	2.9	3.4	2.8	3.1	2.1
	sh*Ltb4r1*	2.0	1.9	1.5	1.9	2.8	2.7	1.8	2.5	1.9

Fig. 5. Blocking LTB_4 during initial lymphangiogenesis period abrogates the therapeutic benefit of LTB_4 antagonism. (**A** to **E**) Serial tail volume measurements of conditions with LTB_4 antagonism before initial lymphangiogenesis period: *Alox5*$^{-/-}$ mice (n = 25) (A), *Ltb4r1*$^{-/-}$ mice (n = 10) (B), WT mice treated with sh*Ltb4r1* lentivirus on day(−7) (sh*Ltb4r1* pretx, n = 8) (C), and WT animals treated with bestatin started on day 0 (bestatin pretx, n = 6) (D) or with Ly293111 started on day 0 (Ly293111 pretx, n = 6) (E). (**F** and **G**) Quantification of dermal thickness (F) and lymphatic area (G) in the day 24 tail skin for (A) to (E); n = 5. (**H**) Quantitations of tail volume on postsurgical day 24 for various groups. (**I**) Relative mRNA expression of key lymphangiogenic factors in the mouse tail skin harvested on day 24 were measured by qRT-PCR. Results were normalized to the saline-treated group. Green indicates an increased average fold change; red indicates a decreased fold change; n = 5. For (A) to (G), data are presented as means and SEM; for (H), data are presented in box-and-whiskers plots showing minimal to maximal values and all data points; comparisons with the saline-treated groups were made by Kruskal-Wallis test followed by Dunn's multiple comparisons test for post hoc analyses.

Loss of Notch signaling in LECs abrogates the effectiveness of LTB_4 antagonism in experimental lymphedema

It has already been demonstrated that lymphatic-specific *Vegfr3* mutations promote preclinical lymphedema generation (*25*), but LEC-specific *Notch1* deficiency has not been previously investigated in lymphedema. Given the established important role of Notch signaling in lymphatic function (*26*–*30*), we generated *Prox1*-specific *Notch1*-deficient mice ($Notch1^{LECKO}$) and evaluated whether blocking LTB_4 would be effective in reversing postsurgical lymphedema (fig. S14). Without surgery, $Notch1^{LECKO}$ mice had dilated lymphatics compared to WT littermates (Fig. 8A), as shown in previous studies (*26*, *27*, *30*). With lymphatic abrogation, $Notch1^{LECKO}$ mice developed lymphedema accompanied by hypersprouting and enlarged, dysfunctional lymphatic vessels that were unable to take up FITC-dextran (Fig. 8A). Blocking LTB_4 synthesis with bestatin did not result in an improvement in the lymphatic architecture or restore the drainage functionality in the $Notch1^{LECKO}$ mice as compared with WT mice (Fig. 8A). The lymphedema generated in $Notch1^{LECKO}$ mice was refractory to bestatin therapy (Fig. 8, B to D). Transcripts of *Vegfr3* were decreased in the $Notch1^{LECKO}$ mice as compared with controls (Fig. 8E), confirming that VEGFR3 is a direct target of the Notch pathway (*18*). Blocking LTB_4 production increased expression of lymphangiogenic factors *Vegfr3*, *Nrp2*, and *EFNB2* in the WT group but not in the transgenic mice (Fig. 8, E to G). We then profiled NICD and EphrinB2 (protein of *EFNB2*) expression in the lymphatics of the $Notch1^{LECKO}$ mice. NICD and EphrinB2 were decreased in the WT mice with lymphedema, indicating a defective Notch pathway associated with pathological changes in the lymphatics (fig. S15A). Immunofluorescence staining of these two proteins demonstrated weak intensity in the $Notch1^{LECKO}$ mice due to the *Notch1* genetic deletion in the LEC. Bestatin did not restore NICD or EphrinB2 expression in $Notch1^{LECKO}$ mice, in contrast to the WT mice (fig. S15, A and B). Because lymphatic Notch pathway is essential to the integrity of functional vessels (*26*, *27*), we next examined the mural smooth muscle coverage of collecting/precollecting lymphatics. Mural coverage of lymphatic vessels, illustrated by the α-smooth muscle actin staining, was not restored by bestatin therapy in $Notch1^{LECKO}$ mice as it was in WT mice (fig. S15, A and B). Bestatin limited tail skin inflammation but did not prevent the enhanced microvascular permeability of $Notch1^{LECKO}$ mice (fig. S16). Furthermore, treatment of DAPT along with bestatin abrogated the therapeutic benefit of bestatin in WT mice with lymphedema (fig. S17). Collectively, these in vivo findings demonstrate that Notch signaling in LEC is required for LTB_4 blockade to restore lymphatic health in acquired lymphedema.

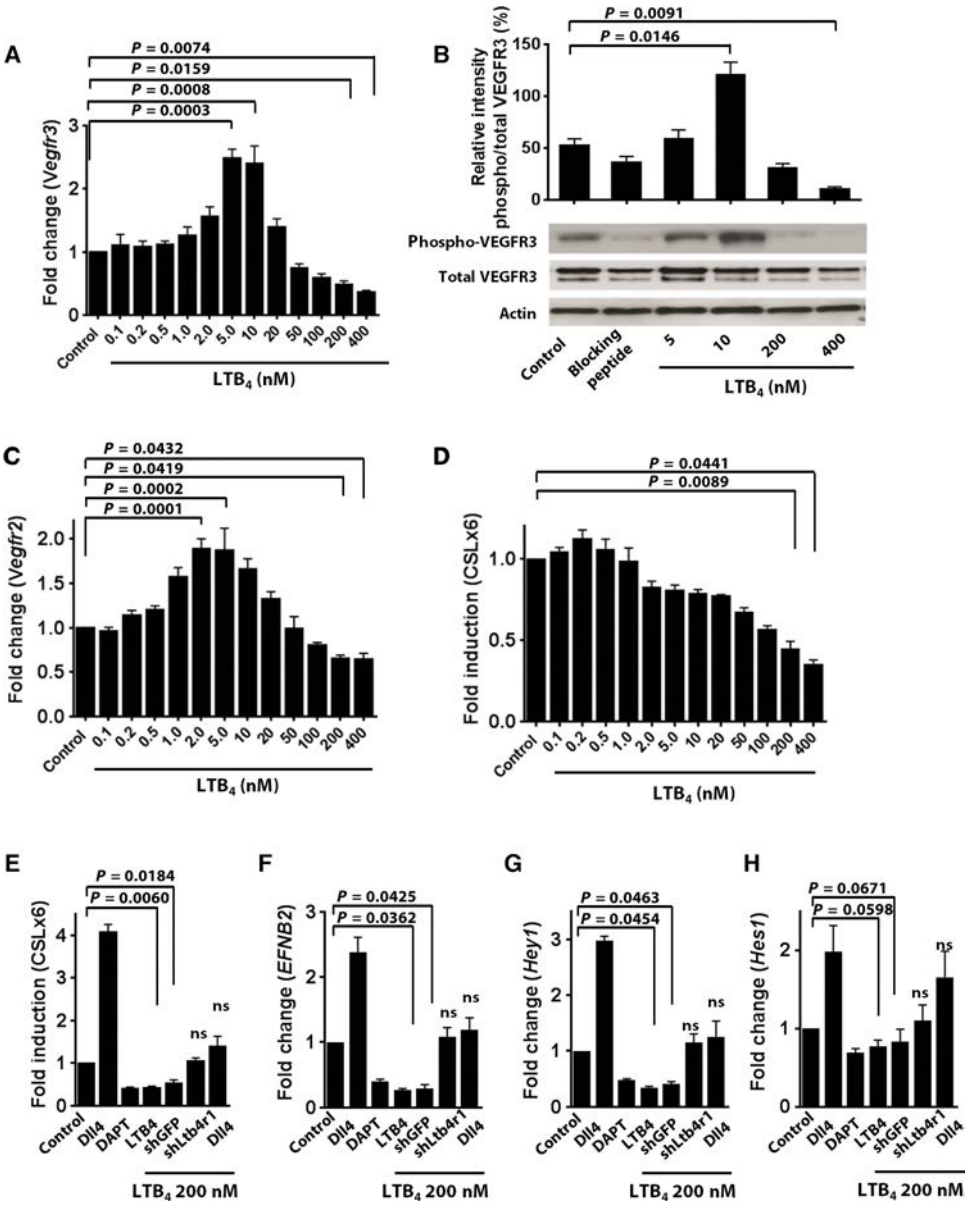

Fig. 6. LTB_4 exerts concentration-dependent effects on VEGFR3 and Notch signaling. (**A**) qRT-PCR analysis measured the relative transcripts of *Vegfr3* in HLECs after the treatment of LTB_4; $n = 5$. (**B**) Western blots detecting phospho-VEGFR3 and total VEGFR3 in HLECs; $n = 3$. (**C**) qRT-PCR analysis measured the relative transcription of *Vegfr2* in HLECs after the treatment of LTB_4; $n = 5$. (**D**) Luciferase activity of HLECs cotransfected with Notch reporter plasmid pG13-11-CSL and pRL-SV40; $n = 5$. Luciferase activity (**E**) or relative transcript expression of *EFNB2*, *Hes1*, and *Hey1* in HLECs (**F** to **H**) was subjected to the treatment of recombinant Dll4 (50 μg/ml; Notch ligand), 25 μM DAPT (Notch inhibitor), 200 nM LTB_4, 200 nM LTB_4 + sh*Ltb4r1*, or 200 nM LTB_4 + Dll4 (50 μg/ml); $n = 5$. All data are presented as means and SEM; comparisons with the control groups were made using Kruskal-Wallis test followed by Dunn's multiple comparisons test for post hoc analyses.

DISCUSSION

Lymphedema is a common, serious, and progressive disease that lacks pharmacologic therapies. Ketoprofen is currently being evaluated clinically as a new therapy for this condition. However, given the

potential toxicities of this NSAID, in the current set of investigations, we sought to elucidate the therapeutic mechanism of action of ketoprofen, to identify a more narrowly targeted and safer treatment approach to lymphedema. Here, we first determined that the efficacy of ketoprofen is attributable to the blockade of LTB_4 biosynthesis and that more targeted LTB_4 antagonism was sufficient to effectively reverse edema and restore lymphatic function. Next, we discovered that LTB_4 has differential, concentration-dependent effects on lymphatic function and on signaling pathways relevant to lymphedema pathogenesis. LTB_4 concentrations were increased in both murine experimental and human clinical lymphedema, and at antilymphangiogenic concentrations, LTB_4 inhibited VEGFR3 and Notch signaling pathways in cultured HLECs. Furthermore, the efficacy of LTB_4 blockade in ameliorating lymphedema required activated lymphatic Notch signaling. These studies provide new biological insights and suggest a new approach for lymphedema treatment. Consequently, a clinical trial of bestatin (Ubenimex) for the treatment of secondary lymphedema was initiated in 2016 (NCT02700529; ULTRA Trial, Eiger BioPharmaceuticals).

Here, bestatin was as effective as ketoprofen and with significantly less adverse effects. In Japan, bestatin has a 35-year history of safety and high tolerability as a chemotherapy adjuvant for leukemia. Its choice as a therapeutic agent may also be favored through its more selective action against LTB_4 biosynthesis. By contrast, ketoprofen is a dual functional inhibitor of both the 5-LO and COX pathways. Blocking COX may have counterproductive effects in lymphedema treatment of cancer survivors because PGE_2, a COX metabolite, actually promotes tumor lymphangiogenesis (*31*, *32*). Accordingly, in our study, ibuprofen, which selectively blocks COX1/2, was ineffective for treating lymphedema; this result suggests that a 5-LO metabolite is responsible for ketoprofen's therapeutic properties, and subsequent interrogation strongly implicates LTB_4 as the most important drug target. The failure of the two other anti-inflammatory agents, ibuprofen and montelukast, suggested that there was a specific role for LTB_4 in lymphedema pathogenesis beyond its role as a leukocyte attractant.

Our group recently reported that LTB_4 induces pulmonary artery endothelial cell apoptosis in a concentration-dependent manner with potential importance in the vascular remodeling observed in pulmonary arterial hypertension (*13*); blocking LTB_4 limited the number and activation of infiltrating macrophages, reduced endothelial injury, and reopened occluded vessels. Similarly, in the current study, bestatin limited macrophage inflammation and decreased tail microvascular permeability. Future studies will pursue how LTB_4 antagonism may alter the phenotype of

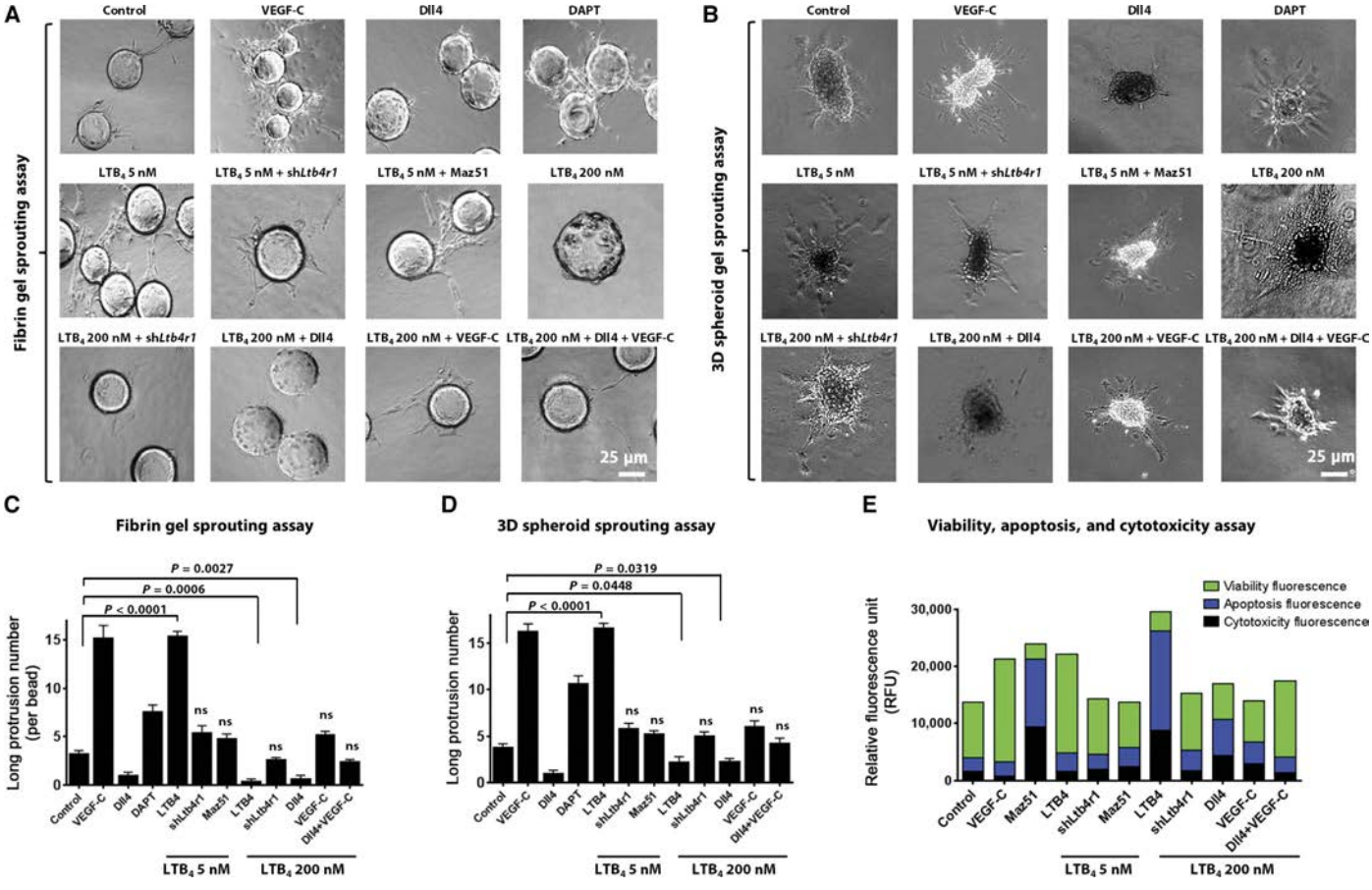

Fig. 7. Bimodal effects of LTB_4 on lymphangiogenesis are regulated by VEGFR3 and Notch signaling. (**A** to **D**) Representative fibrin gel and 3D spheroid sprouting assay images (A and B) and quantification of bimodal effects of LTB_4 on HLEC lymphangiogenesis through regulation of VEGFR3 and Notch signaling (C and D). HLECs were treated with VEGF-C (50 ng/ml), recombinant Dll4 (50 μg/ml), 25 μM DAPT, 5 nM LTB_4, 5 nM LTB_4 + sh*Ltb4r1*, 5 nM LTB_4 + 5 μM MAZ 51(VEGFR3 inhibitor), 200 nM LTB_4, 200 nM LTB_4 + sh*Ltb4r1*, 200 nM LTB_4 + Dll4 (50 μg/ml), 200 nM LTB_4 + VEGF-C (50 ng/ml), or 200 nM LTB_4 + Dll4 (50 μg/ml) + VEGF-C (50 ng/ml. Scale bar, 25 μm. Data are presented as means and SEM; n = 5; comparisons with the control group were made using Kruskal-Wallis test followed by Dunn's multiple comparisons test for post hoc analyses. (**E**) HLEC viability, apoptosis, and cytotoxicity. Mean fluorescence readings are presented; n = 3.

macrophages and better delineate $CD68^+$ populations, which can include epidermal dendritic cells. Given that there has been no previous evaluation of LTB_4 on the lymphatic circulation, we conducted a concentration-dependent study of LTB_4 in several lymphangiogenesis assays. We discovered that LTB_4 had both beneficial and harmful concentration-dependent effects on LECs. The effects of LTB_4 on chemotaxis and cell growth are similarly concentration-dependent (*33*–*36*). LTB_4 exerts its peak chemoattractant effects on monocytes and neutrophils at the same concentration at which it promoted lymphangiogenesis in the current investigation (~10 nM), with a notable falloff in potency at lower and higher concentrations (*33*, *34*). In atherosclerosis, LTB_4 promotes smooth muscle cell chemotaxis at 10 to 100 nM, with reduced effects noted below 10 and above 100 nM (*35*). Likewise, LTB_4 enhances proliferation of colon cancer cells at 10 to 100 nM but not at 0.1 or 1000 nM (*36*). Here, LTB_4 at higher concentrations did not merely lose the prolymphangiogenic action observed at low concentrations but actually gained a deleterious antilymphangiogenic action. We speculate that an important function of LTB_4 in the 10 nM range is to promote angiogenesis/lymphangiogenesis in the initial wound-healing period. The recruitment of angiogenic/lymphangiogenic macrophages is a key component of the wound repair response in this mouse tail model of lymphedema (*37*), and the absence of macrophages alone resulted in poor preclinical outcome; this may contribute to the poor early wound healing observed in bestatin-treated mice (*18*). We suggest that lymphedema develops when an ongoing invasion and accumulation of inflammatory cells generate an environment where concentrations of LTB_4 progressively exceed the prolymphangiogenic range and assume a countervailing deleterious role. LTB_4 not only has direct effects on the lymphatics and microvasculature but clearly promotes inflammation in the affected lymphatic bed; blocking LTB_4 biosynthesis skews the immune response toward an anti-inflammatory response characterized by increased IL-10 production. However, our data suggest that the beneficial properties of LTB_4 antagonism in treating lymphedema extend to actually restoring the lymphatic architecture and function. Because other anti-inflammatory agents, such as ibuprofen and a soluble form of the tumor necrosis factor–α receptor, also limit microvascular permeability without resolving lymphedema, it is unlikely that blocking inflammation alone is sufficient to reverse disease (*4*, *38*, *39*).

Knockout mice ($Alox5^{-/-}$ and $Ltb4r1^{-/-}$) and WT animals pretreated with LTB_4 antagonists were not protected from the development of lymphedema. Our data suggest that in the first few days after surgery, low concentrations of LTB_4 are important in promoting early lymphatic repair, and thus, attempts to antagonize its action are biologically deleterious. However, when tissue LTB_4 concentrations increase into the

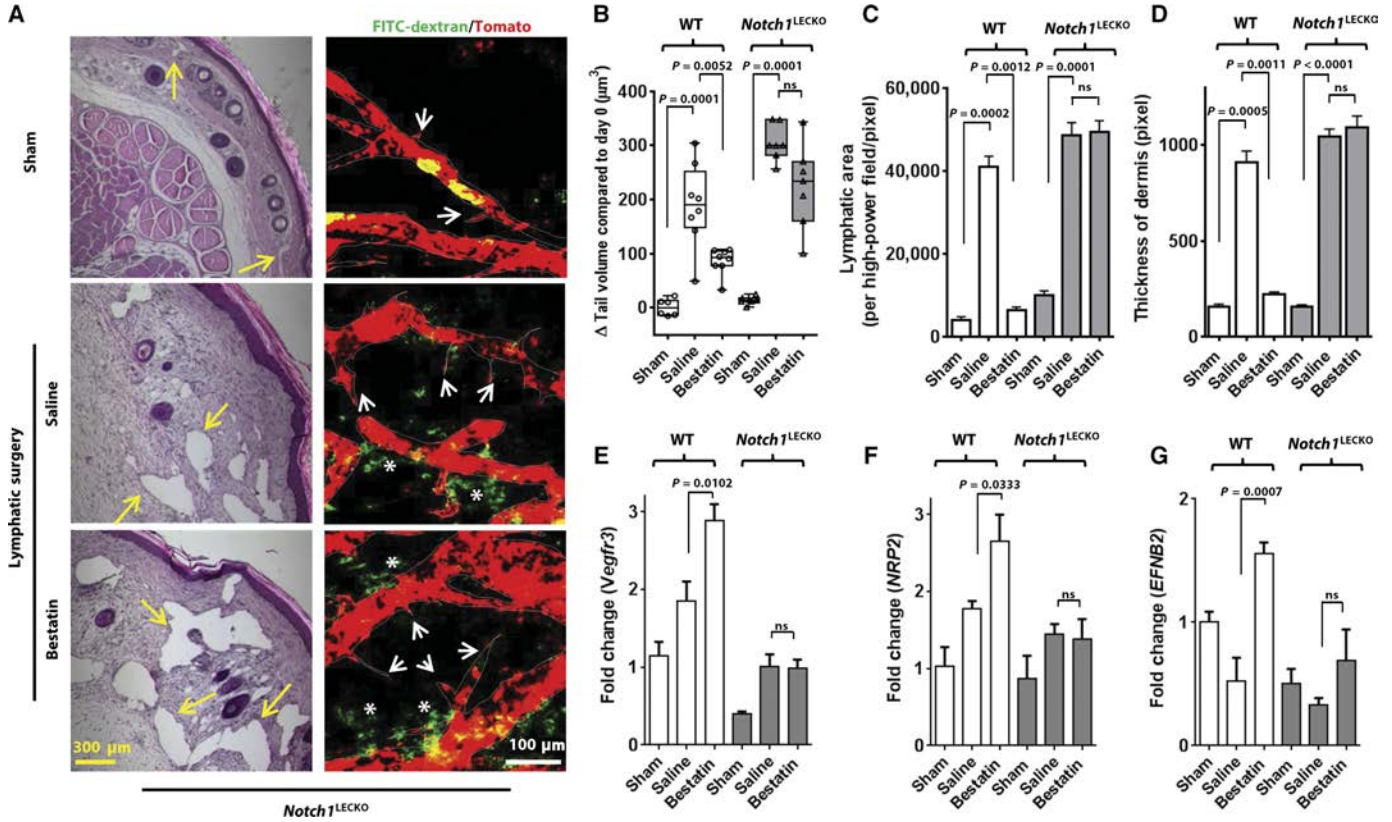

Fig. 8. Loss of Notch signaling in LECs abrogates effectiveness of LTB_4 antagonism in experimental lymphedema. (**A**) Representative histology and fluorescence microlymphangiography of mouse tails of the lymphatic endothelial cell-specific, *Notch1*-deficient ($Notch1^{LECKO}$) mice after sham or lymphatic ablation surgery. Lymphatic dilation is indicated by yellow arrow. Lymphatics are marked by tdTomato and outlined with a white dashed line. FITC-dextran is shown in green. FITC-dextran not taken up by lymphatics is indicated by a white asterisk. White arrowheads point at vessel hypersprouting. Scale bars, 300 or 100 μm, as indicated; $n = 5$. (**B**) Day 24 tail volume measurements of $Notch1^{LECKO}$ mice subjected to lymphatic ablation surgery, treated with saline ($n = 7$) or bestatin ($n = 7$), compared with sham controls ($n = 7$). Quantification of dermal skin thickness (**C**) and lymphatic dilation (**D**) of WT or $Notch1^{LECKO}$ mice in (B); $n = 5$. (**E** to **G**) Relative whole-tail gene transcripts of *Vegfr3* (E), *NRP2* (F), and *EFNB2* (G) of WT or $Notch1^{LECKO}$ mice in (B); $n = 5$. For (B), data are presented in box-and-whiskers plots showing minimal to maximal values and all data points; for (C) to (G), data are presented as means and SEM; Kruskal-Wallis test followed by Dunn's multiple comparisons test for post hoc analyses.

antilymphangiogenic range during evolution of experimental lymphedema, the benefits conferred by LTB_4 are superseded by injury-inducing properties. Intervening at this point with an LTB_4 antagonist can then elicit marked beneficial therapeutic effects, with reversal of lymphedema pathology.

To explain why the 10 nM range LTB_4 was prolymphangiogenic and the ≥200 nM LTB_4 was antilymphangiogenic, we investigated two signaling pathways essential for lymphatic growth: VEGFR3 and Notch. VEGF-C–mediated signaling through VEGFR3 is the major molecular determinant of postnatal lymphangiogenesis and LEC survival. As an example, missense mutations in the tyrosine kinase domain of VEGFR3 are recognized to be responsible for ~70% of cases of autosomal dominant congenital lymphedema (*40*, *41*). Additionally, the therapeutic, lymphangiogenic potential of VEGF-C has been explored in various experimental lymphedema models (*25*, *42*–*44*). Our data indicate that LTB_4 exhibits a dose-dependent regulation of VEGFR3 in HLECs. In the 10 nM range, LTB_4 increased VEGFR3 mRNA and protein expression, sprouting lymphangiogenesis and LEC survival. Conversely, in the ≥200 nM range, LTB_4 significantly inhibited lymphangiogenesis and induced LEC apoptosis through down-regulation of VEGFR3; blocking LTB_4 signaling, through receptor antagonism, restored VEGFR3 expression and normalized LEC sprouting and viability. Furthermore, in experimental lymphedema, blocking LTB_4 production with bestatin increased tissue *Vegfr3* transcript and promoted physiological lymphatic repair.

The mechanisms through which LTB_4 regulates VEGFR3 signaling are still unknown. As shown in the current study, blocking LTB_4 during the prolymphangiogenic phase leads to reduction in *Nrp1*/2 transcripts [VEGF-C co-receptors that regulate VEGFR3 activation (*17*, *45*, *46*)], whereas antagonizing LTB_4 during the antilymphangiogenic phase results in increased *Nrp1*/2 transcripts. These data suggest that LTB_4 could potentially mediate VEGFR3 signaling through regulation of neuropilin. Additionally, 200 nM of LTB_4 is an agonist of peroxisome proliferator–activated receptor γ (PPARγ) (*47*–*49*), a nuclear receptor triggering signaling pathways that inhibit angiogenesis and induce endothelial cell apoptosis, at least partially through its suppression of VEGFR2 and VEGFR3 signaling (*50*). Therefore, it is plausible that at these toxic concentrations, LTB_4 inhibits VEGFR3 expression in LECs through modulation of PPARγ.

Although signaling via VEGF-C/VEGFR3 is perhaps the most central pathway for lymphangiogenesis, a defined role for Notch signaling in lymphatic growth has recently emerged (*23*, *26*–*30*). Notch signaling directly induces VEGFR3 by binding and transactivating the VEGFR3 promoter and thereby promotes endothelial cell survival and morphological changes in response to VEGF-C (*18*). EphrinB2, a Notch target protein, induces the internalization of VEGFR3, thus promoting lymphangiogenesis and LEC growth (*51*), whereas Hey1 and Hes1 suppress VEGFR3 expression and restrain angiogenesis (*22*, *52*). In blood vascular endothelial cells, Notch alters the balance of VEGFR2 and VEGFR3 to facilitate productive angiogenesis and participates in the cell fate determination steps (*19*–*21*, *23*). Within LECs, Notch modulates VEGFR3 expression (*18*, *53*), restrains lymphatic sprouting (*23*), suppresses cellular proliferation, and promotes LEC survival (*26*, *27*). Notch also has been observed to participate in both developmental and postnatal lymphangiogenesis in vivo, wherein reduced Notch activity is associated with defective lymphatic valves (*26*, *27*), immature gut–associated lymphoid tissue (*28*), decreased lymphatic density (sprouting and tip cell morphology) (*30*), compromised mural cell coverage (*27*), and reduced continuous regeneration of lacteals (small intestinal lymphatic capillaries) (*29*). Collectively, these findings indicate an essential role for Notch in developmental and postnatal generation and maintenance of lymphatic vascular structure; they also suggest a potential function of Notch in the reparative responses to lymphatic injury. We demonstrated here that LTB_4, at pathological concentrations, inhibited HLEC Notch signaling in vitro. In lymphedema, decreased Notch activity was associated with elevated LTB_4 production. Pharmacologic blockade of LTB_4 production in mice normalized the tissue expression of NICD and EphrinB2. This mechanism is further supported by our observation that loss of Notch1 activity in *Prox1*-positive LECs in mice abrogated the effectiveness of LTB_4 antagonism. We documented reduced *Vegfr3* transcripts in the $Notch1^{LECKO}$ mice. LTB_4 antagonism restored *Vegfr3* expression in the WT lymphedema mice but not in the $Notch1^{LECKO}$ mice. These observations support the speculation that LTB_4 inhibits HLEC VEGFR3 expression through down-regulation of Notch signaling. Notch signaling also plays a fundamental role in cell fate determination (*54*, *55*). However, in the current study, we were unable to determine whether high concentrations of LTB_4 alter the maintenance of lymphatic identity. Together, our study identifies a novel mechanism through which LTB_4 regulates LEC function, at least in part, by modulating Notch signaling and, thus, the concept that Notch pathway is required for the restoration of a normal lymphatic circulation through LTB_4 antagonism. Whether the VEGFR3 and Notch effects of LTB_4 are dependent or independent events will require further investigation.

Several limitations of the current study should be considered. The tail model of acquired lymphedema likely does not replicate all features of the acquired clinical disease because human pathology typically evolves after lymph node excision that accompanies the traumatic disruption of the vascular channels. The biological concepts elucidated here can be further investigated in alternate disease models, such as the mouse mastectomy model (*44*). Another potential limitation of this study is a possibly incomplete view of LTB_4 action in vivo, and it is certainly possible that some findings attributed to the blockade of LTB_4 may involve other pathways. For example, prolymphangiogenic PGE_2 biosynthesis is up-regulated after LTB_4 blockade, and this provides an additional explanation for disease resolution. Arguing against this possibility, however, is that PGE_2 also induces highly permeable lymphatics and blood vessels, findings not observed with LTB_4 blockade (*56*, *57*). Our initial focus has been on the most well-understood actions of ketoprofen in arachidonic acid metabolism, but the possibility remains that simultaneous blockade of 5-LO and COX1/2 pathways may also induce protective anti-inflammatory eicosanoids, such as lipoxin A_4 or the generation of regulatory T cells (*58*, *59*). We documented that bestatin changed the cytokine profile in the $Notch1^{LECKO}$ differently as compared to the WT littermates. Because Notch is an important regulator of immune cell differentiation and activation and because Notch inhibition markedly affects T helper cell 1 (T_H1), T_H2, and T_H17 responses (*60*–*63*), it can be challenging to explain the differences between groups, and in vivo gene knockout studies can help delineate how Notch suppression specifically contributes to lymphedema-associated inflammation.

In summary, we reported a novel function for LTB_4 in the pathogenesis of lymphedema, documented that LTB_4 exhibited concentration-dependent effects on HLEC function and survival, and demonstrated that LTB_4 antagonism was an effective treatment in the murine tail model of acquired lymphedema. LTB_4 antagonism may thus represent a promising approach in a disease that is currently in need of medical therapies. There is a significant unmet medical need for pharmacologic interventions for this common, serious, and life-altering disease. Enhanced mechanistic insights into the ways in which unchecked inflammation contributes to lymphatic pathology should facilitate new therapeutic discoveries.

MATERIALS AND METHODS

Study design

The sample size of various animal experiments and human tests was determined using a power and sample size calculator (https://www.statisticalsolutions.net/pssZtest_calc.php) to power a study over 80% ($\beta \leq 0.20$). Exclusion criteria were preestablished on the basis of the years of observation while optimizing the animal protocol. Briefly, mice were excluded for analysis if any of the following occurs after surgery: (i) self-inflicted mutilation or severe abrasion on the skin, (ii) severe infection, (iii) loss of blood supply in the tail, and (iv) failure to exceed a 10 to 15% growth in edema by day 3 if no drug was given for lymphedema mice. Animals were randomly allocated to experimental groups and processed using Excel random number generator. Histological analysis and tail volume measurements and quantification were done blindly. Primary data are in the Supplementary Materials (table S3).

Human samples

All studies were approved by the Stanford University Institutional Review Board (protocol #7781). Adult patients with a spectrum of acquired and primary lymphedema were assessed in this study, including those with upper and lower extremity edema, both related and unrelated to a cancer diagnosis. Healthy sex- and age-matched control samples were also used for experiments herein.

Animals

All animal studies were approved by the Administrative Panel on Laboratory Animal Care at Stanford University (APLAC 27376).

Surgical induction of experimental lymphatic vascular insufficiency

Acquired lymphedema was surgically induced in the tails of female C57BL/6J mice through the thermal ablation of lymphatic trunks (lymphatic surgery), using a protocol that has been previously developed and optimized (*4*, *10*). Briefly, a full-thickness circumferential incision of the skin was made 16 mm distal to the base of the mouse tail under anesthesia. Lymphatic trunks were ablated through controlled, limited cautery application under a surgical microscope. For surgical controls (sham surgery and sham), the skin incision alone was performed without lymphatic cautery. All small-molecule drugs were administered through daily intraperitoneal injection. The dosing regimen for each individual drug was as follows: ketoprofen, 5 mg/kg; zileuton, 60 mg/kg; ibuprofen, 5 mg/kg; bestatin, 4 mg/kg; Ly293111, 1 mg/kg; montelukast, 20 mg/kg; and DAPT, 30 mg/kg.

Tail volume quantitation

Tail volume measurements at each designated time were quantified by observers blinded to the treatment status of the subjects. Tail volumes were calculated through a digital photographic technique preoperatively, and postoperatively (days 3, 9, 14, 20, and 24), using an Olympus D-520 Zoom digital camera at super high–quality resolution at a fixed distance from the subject (37 cm), as previously described (*4*, *10*). Tail volumes were derived from the measurement of the tail diameter using the truncated cone approximation (*64*).

Analysis of lymphatic drainage

Lymphatic drainage was analyzed by fluorescence microlymphangiography. Briefly, FITC (0.5 mg/ml)–labeled dextran (molecular weight, 2,000,000; Sigma) was injected intradermally into the tip of the mouse tail at a constant pressure. Fluorescence images of the whole-mount samples were captured using Zeiss 710 confocal microscopy.

Determination of collecting lymphatic transportation function with NIR imaging system

Detailed procedures were described previously (*11*, *12*). Briefly, the effective lymphatic transportation function is characterized using a NIR lymphatic imaging system integrated with a controlled pressure cuff to modulate lymph flow. The collecting lymphatic function was tracked throughout the procedure by imaging the transportation of a NIR tracer injected intradermally, IRDye 800CW NHS ester, at the tip of the mouse tail. A gradual clearance of the lymph flow within the proximal collecting lymphatic occurred when the pressure cuff was inflated (flow clearance phase). NIR labeled lymph flow could then travel beyond the surgical wound through the collecting lymphatic duct because the pressure cuff was sufficiently deflated (flow restoration phase). Trafficking ability of collecting lymphatics in the mouse tail was quantified as the rate of NIR fluorescence movement, calculated using customized algorithms written in MATLAB.

Assessment of lymphatic leakiness

Anesthetized adult mice were injected with a total of 50 μl of 1.0% Evans Blue under skin about 1 cm from the tip of the tail. Skin was gently removed to make windows for the lymphatics on the proximal and distal side of the ligation. Colored by dye, lymphatic vessels were located from the caudal vein and carefully dissected for imaging.

Statistics

GraphPad Prism version 5.0c was used for statistical analysis. Differences between two groups at a single time point were compared using Mann-Whitney test. For comparisons between multiple experimental groups at a single time point, Kruskal-Wallis test followed by Dunn's multiple comparisons test for post hoc analyses were used. Pearson correlation test was used to calculate linear regression. All analyses were considered statistically significant at $P < 0.05$.

SUPPLEMENTARY MATERIALS

www.sciencetranslationalmedicine.org/cgi/content/full/9/389/eaal3920/DC1

Materials and Methods

Fig. S1. Mouse tail model of acquired lymphedema.

Fig. S2. Analysis of mouse tail edema and LTB_4 and BLT1 expression after LTB_4 antagonism started on postoperative day 3.

Fig. S3. Bestatin treatment reduces inflammation.

Fig. S4. Macrophage depletion does not resolve mouse tail lymphedema.

Fig. S5. Bestatin treatment reduces microvascular permeability in mouse tail lymphedema.

Fig. S6. LTB_4 inhibits in vivo and in vitro HLEC lymphangiogenesis.

Fig. S7. LTB_4 (400 nM) damages HLEC junctions and reduces connexin mRNA transcript.

Fig. S8. 5-LO expression in neutrophils and macrophages is increased in human lymphedema.

Fig. S9. Increased LTB_4 and decreased PGE2 signaling in mouse tail lymphedema.

Fig. S10. LTB_4 antagonism before initial lymphangiogenesis period is not therapeutic.

Fig. S11. LTB_4 exerts concentration-dependent effects on HLEC VEGFR2 signaling.

Fig. S12. Overexpressing 5-LO interferences lymphatic drainage and promotes microvascular leakage in mouse tail.

Fig. S13. LTB_4 (200 nM) inhibits Notch signaling in HLECs.

Fig. S14. Confirmation of the generation of Prox1-specific, Notch1-deficient ($Notch1^{LECKO}$) mice.

Fig. S15. Bestatin does not rescue Notch signaling or limit lymphatic dilation in $Notch1^{LECKO}$ mice.

Fig. S16. Effects of bestatin on inflammation and microvascular permeability in *Notch1*^{LECKO} mice.

Fig. S17. Bestatin does not rescue tail lymphedema in mice treated with DAPT.

Table S1. Demographics of healthy controls and lymphedema patients—LTB_4 and PGE_2 analysis.

Table S2. Summary of lymphangiogenesis and angiogenesis microarray results.
Table S3. Primary data.
Movie S1. NIR imaging of collecting lymphatics in the healthy control mouse.
Movie S2. NIR imaging of collecting lymphatics in the bestatin-treated mouse after lymphatic ablation surgery.
Movie S3. NIR imaging of collecting lymphatics in the saline-treated mouse after lymphatic ablation surgery.

REFERENCES AND NOTES

1. E. D. Paskett, J. A. Dean, J. M. Oliveri, J. P. Harrop, Cancer-related lymphedema risk factors, diagnosis, treatment, and impact: A review. *J. Clin. Oncol.* **30**, 3726–3733 (2012).
2. S. G. Rockson, Update on the biology and treatment of lymphedema. *Curr. Treat. Options Cardiovasc. Med.* **14**, 184–192 (2012).
3. S. G. Rockson, Diagnosis and management of lymphatic vascular disease. *J. Am. Coll. Cardiol.* **52**, 799–806 (2008).
4. K. Nakamura, K. Radhakrishnan, Y. M. Wong, S. G. Rockson, Anti-inflammatory pharmacotherapy with ketoprofen ameliorates experimental lymphatic vascular insufficiency in mice. *PLOS ONE* **4**, e8380 (2009).
5. J. L. Ambrus Jr., S. Haneiwich, L. Chesky, P. McFarland, R. J. Engler, Improved in vitro antigen-specific antibody synthesis in two patients with common variable immunodeficiency taking an oral cyclooxygenase and lipoxygenase inhibitor (ketoprofen). *J. Allergy Clin. Immunol.* **88**, 775–783 (1991).
6. W. Dawson, J. R. Boot, J. Harvey, J. R. Walker, The pharmacology of benoxaprofen with particular to effects on lipoxygenase product formation. *Eur. J. Rheumatol. Inflamm.* **5**, 61–68 (1982).
7. Z. Rajić, D. Hadjipavlou-Litina, E. Pontiki, M. Kralj, L. Šuman, B. Zorc, The novel ketoprofen amides—Synthesis and biological evaluation as antioxidants, lipoxygenase inhibitors and cytostatic agents. *Chem. Biol. Drug Des.* **75**, 641–652 (2010).
8. M. Peters-Golden, W. R. Henderson Jr., Leukotrienes. *N. Engl. J. Med.* **357**, 1841–1854 (2007).
9. M. Schneider, A. Ny, C. Ruiz de Almodovar, P. Carmeliet, A new mouse model to study acquired lymphedema. *PLOS Med.* **3**, e264 (2006).
10. R. Tabibiazar, L. Cheung, J. Han, J. Swanson, A. Beilhack, A. An, S. S. Dadras, N. Rockson, S. Joshi, R. Wagner, S. G. Rockson, Inflammatory manifestations of experimental lymphatic insufficiency. *PLOS Med.* **3**, e254 (2006).
11. T. S. Nelson, R. E. Akin, M. J. Weiler, T. Kassis, J. A. Kornuta, J. B. Dixon, Minimally invasive method for determining the effective lymphatic pumping pressure in rats using near-infrared imaging. *Am. J. Physiol. Regul. Integr. Comp. Physiol.* **306**, R281–R290 (2014).
12. M. Weiler, J. B. Dixon, Differential transport function of lymphatic vessels in the rat tail model and the long-term effects of Indocyanine Green as assessed with near-infrared imaging. *Front. Physiol.* **4**, 215 (2013).
13. W. Tian, X. Jiang, R. Tamosiuniene, Y. K. Sung, J. Qian, G. Dhillon, L. Gera, L. Farkas, M. Rabinovitch, R. T. Zamanian, M. Inayathullah, M. Fridlib, J. Rajadas, M. Peters-Golden, N. F. Voelkel, M. R. Nicolls, Blocking macrophage leukotriene B_4 prevents endothelial injury and reverses pulmonary hypertension. *Sci. Transl. Med.* **5**, 200ra117 (2013).
14. J. M. Rutkowski, K. C. Boardman, M. A. Swartz, Characterization of lymphangiogenesis in a model of adult skin regeneration. *Am. J. Physiol. Heart Circ. Physiol.* **291**, H1402–H1410 (2006).
15. T. Lämmermann, P. V. Afonso, B. R. Angermann, J. M. Wang, W. Kastenmüller, C. A. Parent, R. N. Germain, Neutrophil swarms require LTB4 and integrins at sites of cell death in vivo. *Nature* **498**, 371–375 (2013).
16. M. K. Oyoshi, R. He, Y. Li, S. Mondal, J. Yoon, R. Afshar, M. Chen, D. M. Lee, H. R. Luo, A. D. Luster, J. S. Cho, L. S. Miller, A. Larson, G. F. Murphy, R. S. Geha, Leukotriene B4-driven neutrophil recruitment to the skin is essential for allergic skin inflammation. *Immunity* **37**, 747–758 (2012).
17. W. Zheng, A. Aspelund, K. Alitalo, Lymphangiogenic factors, mechanisms, and applications. *J. Clin. Invest.* **124**, 878–887 (2014).
18. C. J. Shawber, Y. Funahashi, E. Francisco, M. Vorontchikhina, Y. Kitamura, S. A. Stowell, V. Borisenko, N. Feirt, S. Podgrabinska, K. Shiraishi, K. Chawengsaksophak, J. Rossant, D. Accili, M. Skobe, J. Kitajewski, Notch alters VEGF responsiveness in human and murine endothelial cells by direct regulation of VEGFR-3 expression. *J. Clin. Invest.* **117**, 3369–3382 (2007).
19. I. Noguera-Troise, C. Daly, N. J. Papadopoulos, S. Coetzee, P. Boland, N. W. Gale, H. C. Lin, G. D. Yancopoulos, G. Thurston, Blockade of Dll4 inhibits tumour growth by promoting non-productive angiogenesis. *Nature* **444**, 1032–1037 (2006).
20. A. F. Siekmann, N. D. Lawson, Notch signalling limits angiogenic cell behaviour in developing zebrafish arteries. *Nature* **445**, 781–784 (2007).
21. M. Hellström, L.-K. Phng, J. J. Hofmann, E. Wallgard, L. Coultas, P. Lindblom, J. Alva, A.-K. Nilsson, L. Karlsson, N. Gaiano, K. Yoon, J. Rossant, M. L. Iruela-Arispe, M. Kalén, H. Gerhardt, C. Betsholtz, Dll4 signalling through Notch1 regulates formation of tip cells during angiogenesis. *Nature* **445**, 776–780 (2007).
22. T. Tammela, G. Zarkada, E. Wallgard, A. Murtomäki, S. Suchting, M. Wirzenius, M. Waltari, M. Hellström, T. Schomber, R. Peltonen, C. Freitas, A. Duarte, H. Isoniemi, P. Laakkonen, G. Christofori, S. Ylä-Herttuala, M. Shibuya, B. Pytowski, A. Eichmann, C. Betsholtz, K. Alitalo, Blocking VEGFR-3 suppresses angiogenic sprouting and vascular network formation. *Nature* **454**, 656–660 (2008).
23. W. Zheng, T. Tammela, M. Yamamoto, A. Anisimov, T. Holopainen, S. Kaijalainen, T. Karpanen, K. Lehti, S. Ylä-Herttuala, K. Alitalo, Notch restricts lymphatic vessel sprouting induced by vascular endothelial growth factor. *Blood* **118**, 1154–1162 (2011).
24. T. Mäkinen, T. Veikkola, S. Mustjoki, T. Karpanen, B. Catimel, E. C. Nice, L. Wise, A. Mercer, H. Kowalski, D. Kerjaschki, S. A. Stacker, M. G. Achen, K. Alitalo, Isolated lymphatic endothelial cells transduce growth, survival and migratory signals via the VEGF-C/D receptor VEGFR-3. *EMBO J.* **20**, 4762–4773 (2001).
25. M. J. Karkkainen, A. Saaristo, L. Jussila, K. A. Karila, E. C. Lawrence, K. Pajusola, H. Bueler, A. Eichmann, R. Kauppinen, M. I. Kettunen, S. Ylä-Herttuala, D. N. Finegold, R. E. Ferrell, K. Alitalo, A model for gene therapy of human hereditary lymphedema. *Proc. Natl. Acad. Sci. U.S.A.* **98**, 12677–12682 (2001).
26. A. Murtomaki, M. K. Uh, C. Kitajewski, J. Zhao, T. Nagasaki, C. J. Shawber, J. Kitajewski, Notch signaling functions in lymphatic valve formation. *Development* **141**, 2446–2451 (2014).
27. A. Murtomaki, M. K. Uh, Y. K. Choi, C. Kitajewski, V. Borisenko, J. Kitajewski, C. J. Shawber, Notch1 functions as a negative regulator of lymphatic endothelial cell differentiation in the venous endothelium. *Development* **140**, 2365–2376 (2013).
28. Y. Obata, S. Kimura, G. Nakato, K. Iizuka, Y. Miyagawa, Y. Nakamura, Y. Furusawa, M. Sugiyama, K. Suzuki, M. Ebisawa, Y. Fujimura, H. Yoshida, T. Iwanaga, K. Hase, H. Ohno, Epithelial–stromal interaction via Notch signaling is essential for the full maturation of gut-associated lymphoid tissues. *EMBO Rep.* **15**, 1297–1304 (2014).
29. J. Bernier-Latmani, C. Cisarovsky, C. S. Demir, M. Bruand, M. Jaquet, S. Davanture, S. Ragusa, S. Siegert, O. Dormond, R. Benedito, F. Radtke, S. A. Luther, T. V. Petrova, DLL4 promotes continuous adult intestinal lacteal regeneration and dietary fat transport. *J. Clin. Invest.* **125**, 4572–4586 (2015).
30. A. Fatima, A. Culver, F. Culver, T. Liu, W. H. Dietz, B. R. Thomson, A.-K. Hadjantonakis, S. E. Quaggin, T. Kume, Murine *Notch1* is required for lymphatic vascular morphogenesis during development. *Dev. Dyn.* **243**, 957–964 (2014).
31. T. R. Lyons, V. F. Borges, C. B. Betts, Q. Guo, P. Kapoor, H. A. Martinson, S. Jindal, P. Schedin, Cyclooxygenase-2–dependent lymphangiogenesis promotes nodal metastasis of postpartum breast cancer. *J. Clin. Invest.* **124**, 3901–3912 (2014).
32. F. Ogawa, H. Amano, K. Eshima, Y. Ito, Y. Matsui, K. Hosono, H. Kitasato, A. Iyoda, K. Iwabuchi, Y. Kumagai, Y. Satoh, S. Narumiya, M. Majima, Prostanoid induces premetastatic niche in regional lymph nodes. *J. Clin. Invest.* **124**, 4882–4894 (2014).
33. T. Ternowitz, T. Herlin, K. Fogh, Human monocyte and polymorphonuclear leukocyte chemotactic and chemokinetic responses to leukotriene B4 and FMLP. *Acta. Pathol. Microbiol. Immunol. Scand. C* **95**, 47–54 (1987).
34. M. A. Shirley, C. T. Reidhead, R. C. Murphy, Chemotactic LTB_4 metabolites produced by hepatocytes in the presence of ethanol. *Biochem. Biophys. Res. Commun.* **185**, 604–610 (1992).
35. E. A. Heller, E. Liu, A. M. Tager, S. Sinha, J. D. Roberts, S. L. Koehn, P. Libby, E. R. Aikawa, J. Q. Chen, P. Huang, M. W. Freeman, K. J. Moore, A. D. Luster, R. E. Gerszten, Inhibition of atherogenesis in BLT1-deficient mice reveals a role for LTB4 and BLT1 in smooth muscle cell recruitment. *Circulation* **112**, 578–586 (2005).
36. C. Bortuzzo, R. Hanif, K. Kashfi, L. Staiano-Coico, S. J. Shiff, B. Rigas, The effect of leukotrienes B and selected HETEs on the proliferation of colon cancer cells. *Biochim. Biophys. Acta* **1300**, 240–246 (1996).
37. S. Ghanta, D. A. Cuzzone, J. S. Torrisi, N. J. Albano, W. J. Joseph, I. L. Savetsky, J. C. Gardenier, D. Chang, J. C. Zampell, B. J. Mehrara, Regulation of inflammation and fibrosis by macrophages in lymphedema. *Am. J. Physiol. Heart Circ. Physiol.* **308**, H1065–H1077 (2015).
38. S. Hofmann, H. Grasberger, P. Jung, M. Bidlingmaier, J. Vlotides, O. E. Janssen, R. Landgraf, The tumour necrosis factor-alpha induced vascular permeability is associated with a reduction of VE-cadherin expression. *Eur. J. Med. Res.* **7**, 171–176 (2002).
39. L.-T. Huang, C.-H. Lin, H.-C. Chou, C.-M. Chen, Ibuprofen protects ventilator-induced lung injury by downregulating Rho-kinase activity in rats. *Biomed. Res. Int.* **2014**, 749097 (2014).
40. M. J. Karkkainen, R. E. Ferrell, E. C. Lawrence, M. A. Kimak, K. L. Levinson, M. A. McTigue, K. Alitalo, D. N. Finegold, Missense mutations interfere with VEGFR-3 signalling in primary lymphoedema. *Nat. Genet.* **25**, 153–159 (2000).
41. A. Irrthum, M. J. Karkkainen, K. Devriendt, K. Alitalo, M. Vikkula, Congenital hereditary lymphedema caused by a mutation that inactivates VEGFR3 tyrosine kinase. *Am. J. Hum. Genet.* **67**, 295–301 (2000).
42. Y.-s. Yoon, T. Murayama, E. Gravereaux, T. Tkebuchava, M. Silver, C. Curry, A. Wecker, R. Kirchmair, C. S. Hu, M. Kearney, A. Ashare, D. G. Jackson, H. Kubo, J. M. Isner, D. W. Losordo, VEGF-C gene therapy augments postnatal lymphangiogenesis and ameliorates secondary lymphedema. *J. Clin. Invest.* **111**, 717–725 (2003).

43. A. Szuba, M. Skobe, M. J. Karkkainen, W. S. Shin, D. P. Beynet, N. B. Rockson, N. Dakhil, S. Spilman, M. L. Goris, H. W. Strauss, T. Quertermous, K. Alitalo, S. G. Rockson, Therapeutic lymphangiogenesis with human recombinant VEGF-C. *FASEB J.* **16**, 1985–1987 (2002).
44. T. Tammela, A. Saaristo, T. Holopainen, J. Lyytikka, A. Kotronen, M. Pitkonen, U. Abo-Ramadan, S. Ylä-Herttuala, T. V. Petrova, K. Alitalo, Therapeutic differentiation and maturation of lymphatic vessels after lymph node dissection and transplantation. *Nat. Med.* **13**, 1458–1466 (2007).
45. Y. Xu, L. Yuan, J. Mak, L. Pardanaud, M. Caunt, I. Kasman, B. Larrivée, R. Del Toro, S. Suchting, A. Medvinsky, J. Silva, J. Yang, J.-L. Thomas, A. W. Koch, K. Alitalo, A. Eichmann, A. Bagri, Neuropilin-2 mediates VEGF-C–induced lymphatic sprouting together with VEGFR3. *J. Cell Biol.* **188**, 115–130 (2010).
46. M. W. Parker, A. D. Linkugel, H. L. Goel, T. Wu, A. M. Mercurio, C. W. Vander Kooi, Structural basis for VEGF-C binding to neuropilin-2 and sequestration by a soluble splice form. *Structure* **23**, 677–687 (2015).
47. V. R. Narala, R. K. Adapala, M. V. Suresh, T. G. Brock, M. Peters-Golden, R. C. Reddy, Leukotriene B_4 is a physiologically relevant endogenous peroxisome proliferator-activated receptor-α agonist. *J. Biol. Chem.* **285**, 22067–22074 (2010).
48. J. Fiedler, F. R. Simon, M. Iwahashi, R. C. Murphy, Effect of peroxisome proliferator-activated receptor α activation on leukotriene B_4 metabolism in isolated rat hepatocytes. *J. Pharmacol. Exp. Ther.* **299**, 691–697 (2001).
49. T. Yokomizo, T. Izumi, K. Chang, Y. Takuwa, T. Shimizu, A G-protein-coupled receptor for leukotriene B_4 that mediates chemotaxis. *Nature* **387**, 620–624 (1997).
50. R. Grau, M. D. Díaz-Muñoz, C. Cacheiro-Llaguno, M. Fresno, M. A. Iniguez, Role of peroxisome proliferator-activated receptor alpha in the control of cyclooxygenase 2 and vascular endothelial growth factor: Involvement in tumor growth. *PPAR Res.* **2008**, 352437 (2008).
51. Y. Wang, M. Nakayama, M. E. Pitulescu, T. S. Schmidt, M. L. Bochenek, A. Sakakibara, S. Adams, A. Davy, U. Deutsch, U. Lüthi, A. Barberis, L. E. Benjamin, T. Mäkinen, C. D. Nobes, R. H. Adams, Ephrin-B2 controls VEGF-induced angiogenesis and lymphangiogenesis. *Nature* **465**, 483–486 (2010).
52. T. Tammela, G. Zarkada, H. Nurmi, L. Jakobsson, K. Heinolainen, D. Tvorogov, W. Zheng, C. A. Franco, A. Murtomaki, E. Aranda, N. Miura, S. Ylä-Herttuala, M. Fruttiger, T. Mäkinen, A. Eichmann, J. W. Pollard, H. Gerhardt, K. Alitalo, VEGFR-3 controls tip to stalk conversion at vessel fusion sites by reinforcing Notch signalling. *Nat. Cell Biol.* **13**, 1202–1213 (2011).
53. R. Benedito, S. F. Rocha, M. Woeste, M. Zamykal, F. Radtke, O. Casanovas, A. Duarte, B. Pytowski, R. H. Adams, Notch-dependent VEGFR3 upregulation allows angiogenesis without VEGF–VEGFR2 signalling. *Nature* **484**, 110–114 (2012).
54. E. Zacharioudaki, B. E. Housden, G. Garinis, R. Stojnic, C. Delidakis, S. J. Bray, Genes implicated in stem cell identity and temporal programme are directly targeted by Notch in neuroblast tumours. *Development* **143**, 219–231 (2016).
55. M. Khacho, A. Clark, D. S. Svoboda, J. Azzi, J. G. MacLaurin, C. Meghaizel, H. Sesaki, D. C. Lagace, M. Germain, M.-E. Harper, D. S. Park, R. S. Slack, Mitochondrial dynamics impacts stem cell identity and fate decisions by regulating a nuclear transcriptional program. *Cell Stem Cell* **19**, 232–247 (2016).
56. K. Omori, T. Kida, M. Hori, H. Ozaki, T. Murata, Multiple roles of the PGE_2-EP receptor signal in vascular permeability. *Br. J. Pharmacol.* **171**, 4879–4889 (2014).
57. K. Morimoto, N. Shirata, Y. Taketomi, S. Tsuchiya, E. Segi-Nishida, T. Inazumi, K. Kabashima, S. Tanaka, M. Murakami, S. Narumiya, Y. Sugimoto, Prostaglandin E_2–EP3 signaling induces inflammatory swelling by mast cell activation. *J. Immunol.* **192**, 1130–1137 (2014).
58. K. Atarashi, T. Mori, R. Yoshiki, K. Kabashima, H. Kuma, Y. Tokura, Skin application of ketoprofen systemically suppresses contact hypersensitivity by inducing $CD4^+$ $CD25^+$ regulatory T cells. *J. Dermatol. Sci.* **53**, 216–221 (2009).
59. E. Gousopoulos, S. T. Proulx, S. B. Bachmann, J. Scholl, D. Dionyssiou, E. Demiri, C. Halin, L. C. Dieterich, M. Detmar, Regulatory T cell transfer ameliorates lymphedema and promotes lymphatic vessel function. *JCI Insight* **1**, e89081 (2016).
60. H. Xu, J. Zhu, S. Smith, J. Foldi, B. Zhao, A. Y. Chung, H. Outtz, J. Kitajewski, C. Shi, S. Weber, P. Saftig, Y. Li, K. Ozato, C. P. Blobel, L. B. Ivashkiv, X. Hu, Notch–RBP-J signaling regulates the transcription factor IRF8 to promote inflammatory macrophage polarization. *Nat. Immunol.* **13**, 642–650 (2012).
61. X. Hu, A. Y. Chung, I. Wu, J. Foldi, J. Chen, J. D. Ji, T. Tateya, Y. J. Kang, J. Han, M. Gessler, R. Kageyama, L. B. Ivashkiv, Integrated regulation of Toll-like receptor responses by Notch and interferon-γ pathways. *Immunity* **29**, 691–703 (2008).
62. F. Radtke, H. R. MacDonald, F. Tacchini-Cottier, Regulation of innate and adaptive immunity by Notch. *Nat. Rev. Immunol.* **13**, 427–437 (2013).
63. K. Piggott, J. Deng, K. Warrington, B. Younge, J. T. Kubo, M. Desai, J. J. Goronzy, C. M. Weyand, Blocking the NOTCH pathway inhibits vascular inflammation in large-vessel vasculitis. *Circulation* **123**, 309–318 (2011).
64. J. Sitzia, Volume measurement in lymphoedema treatment: Examination of formulae. *Eur. J. Cancer Care* **4**, 11–16 (1995).

Acknowledgments: We acknowledge G. C. Oliver, C. Kuo, and T. Reyes for providing the *Prox1-Cre-ERT2* mice. **Funding:** This research was funded by Stanford Startup funds and Endowed Chair funds (M.R.N.). **Author contributions:** W.T., S.G.R., X.J., and J.K. designed research studies, conducted experiments, acquired and analyzed data, and wrote the manuscript. A.B., E.M.S. and A.B.T. conducted experiments, acquired data, and helped write the manuscript. M.C., Z.N., and A.H.F. conducted experiments and acquired and analyzed data. R.T.Z., N.F.V., and M.P.-G. helped write the manuscript. G.S.D. helped analyze data and write the manuscript. J.K. designed research studies, provided reagents, and helped write the manuscript. J.B.D. designed research studies. M.R.N. designed research studies, analyzed data, provided funding, and wrote the manuscript. **Competing interests:** W.T., S.G.R., X.J., J.K., and M.R.N. are inventors on a patent (pending; PCT/US2016/022132) licensed by Eiger BioPharmaceuticals from Stanford University/VA Palo Alto Health Care System that covers LTB_4 inhibition to prevent and treat human lymphedema. W.T. and M.R.N. have equity interest in Eiger BioPharmaceuticals, which develops drugs targeting LTB_4 for the treatment of secondary lymphedema. All other authors declare that they have no competing interests.

Submitted 11 November 2016
Resubmitted 22 November 2016
Accepted 4 April 2017
Published 10 May 2017
10.1126/scitranslmed.aal3920

Citation: W. Tian, S. G. Rockson, X. Jiang, J. Kim, A. Begaye, E. M. Shuffle, A. B. Tu, M. Cribb, Z. Nepiyushchikh, A. H. Feroze, R. T. Zamanian, G. S. Dhillon, N. F. Voelkel, M. Peters-Golden, J. Kitajewski, J. B. Dixon, M. R. Nicolls, Leukotriene B_4 antagonism ameliorates experimental lymphedema. *Sci. Transl. Med.* **9**, eaal3920 (2017).